


REVIEW

Structural mechanisms of transient receptor potential ion channels

Erhu Cao 

Transient receptor potential (TRP) ion channels are evolutionarily ancient sensory proteins that detect and integrate a wide range of physical and chemical stimuli. TRP channels are fundamental for numerous biological processes and are therefore associated with a multitude of inherited and acquired human disorders. In contrast to many other major ion channel families, high-resolution structures of TRP channels were not available before 2013. Remarkably, however, the subsequent “resolution revolution” in cryo-EM has led to an explosion of TRP structures in the last few years. These structures have confirmed that TRP channels assemble as tetramers and resemble voltage-gated ion channels in their overall architecture. But beyond the relatively conserved transmembrane core embedded within the lipid bilayer, each TRP subtype appears to be endowed with a unique set of soluble domains that may confer diverse regulatory mechanisms. Importantly, TRP channel structures have revealed sites and mechanisms of action of numerous synthetic and natural compounds, as well as those for endogenous ligands such as lipids, Ca²⁺, and calmodulin. Here, I discuss these recent findings with a particular focus on the conserved transmembrane region and how these structures may help to rationally target this important class of ion channels for the treatment of numerous human conditions.

Introduction

The transient receptor potential (TRP) ion channels conduct cations and, based on similarity in their primary sequences, are grouped into seven subfamilies: TRPC (canonical), TRPM (melastatin), TRPA (ankyrin), TRPV (vanilloid), TRPN (nomp; absent in mammals), TRPML (mucolipin), and TRPP (polycystin; Ramsey et al., 2006; Venkatachalam and Montell, 2007). The human genome encodes 27 TRP proteins, making them the second largest class of ion channels, surpassed only by K⁺ channels. TRP channels exhibit very low sequence homology across different subfamilies, reflecting their diverse physiological roles as sensory apparatuses that detect and respond to all manner of environmental and physiological stimuli. The first TRP channels (TRP and TRP like [TRPL]) were identified in fly eyes, where they operate downstream of the rhodopsin-phospholipase C pathway and underlie phototransduction (Hardie and Minke, 1993; Montell, 2012). For most mammalian TRP channels, in vivo activation mechanisms remain elusive. However, many of them, like the ancestral fly TRP channels, retain the ability to be regulated by hormones or neurotransmitters that stimulate phospholipase C-coupled receptors.

TRP channels assemble as homo- or heterotetramers with a membrane topology and subunit organization resembling that of

voltage-gated ion channels (VGICs; Fig. 1). The transmembrane core of each TRP subunit harbors two recognizable modules embedded within the lipid bilayer: a voltage sensor-like domain composed of the first four helices (S1–S4; VSLD) and a pore domain formed by the last two helices (S5 and S6) plus the intervening loop. These two modules are connected by the S4–S5 linker, a short amphipathic helix that runs almost parallel to the inner membrane. TRP channels exhibit fourfold symmetry along a central ion permeation pathway formed by pore modules from four subunits. The central pore is flanked by the peripheral VSLDs in a “domain-swap” organization, whereby each VSLD associates with the pore domain from a neighboring subunit, as first observed in voltage-gated K⁺ channels (Long et al., 2005a, 2007; Liao et al., 2013). Of note, the TRPV6 channel, when perturbed either by introducing a single mutation in the S5 helix or by artificially shortening the S4–S5 linker, deviates from this general architecture and surprisingly adopts a “non-swapped” structure (Saotome et al., 2016; Singh et al., 2017). However, whether this “non-swapped” TRPV6 channel exists and functions in native epithelia remains to be determined.

TRP channels generally exhibit modest voltage sensitivity, likely due to a lack of regularly spaced arginine or lysine residues (gating charges) in their S4 helices. Gating charges are a

Department of Biochemistry, University of Utah School of Medicine, Salt Lake City, UT.

Correspondence to Erhu Cao: erhu.cao@biochem.utah.edu.

© 2020 Cao. This article is distributed under the terms of an Attribution–Noncommercial–Share Alike–No Mirror Sites license for the first six months after the publication date (see <http://www.rupress.org/terms/>). After six months it is available under a Creative Commons License (Attribution–Noncommercial–Share Alike 4.0 International license, as described at <https://creativecommons.org/licenses/by-nc-sa/4.0/>).

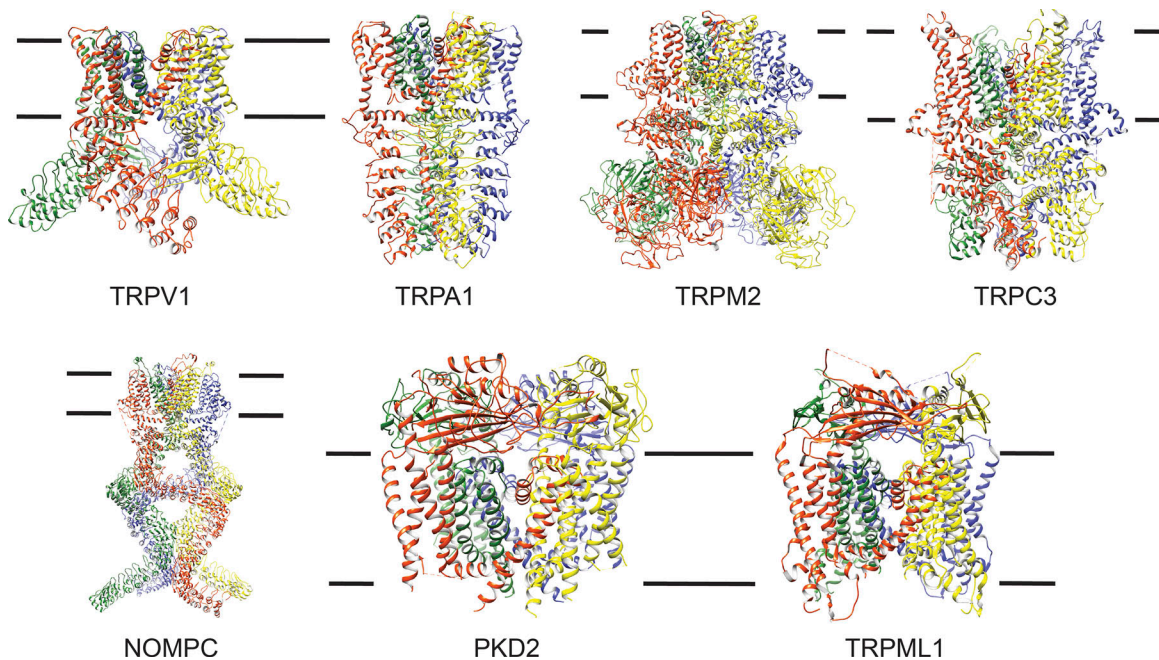


Figure 1. **Representative structures of each of the seven TRP subfamilies.** TRP channels are shown in ribbon diagrams viewed parallel to the membrane, with each subunit color-coded differently. Note, TRP channels are decorated with unique soluble domains outside the relatively conserved transmembrane core structure embedded within the lipid bilayer delimited with two black horizontal lines. PDB accession nos. are as follows: TRPV1 (3J5P), TRPA1 (3J9P), TRPM2 (6MIX), TRPC3 (6CUD), no mechanoreceptor potential C (NOMPC; 5VKQ), PKD2 (5T4D), and TRPML1 (5WJ5).

hallmark of VGICs and enable movement of the S4 helix in accordance with the electric field of the membrane, which in turn is believed to exert force on the S4–S5 linker to ultimately open or close the pore (Long et al., 2005b; Catterall, 2010; Vargas et al., 2012). Notwithstanding this notable difference, VSLDs of TRP channels are coupled to the pore module via the S4–S5 linker (in analogy to VGICs) and, in the case of TRPM4, TRPML1, and TRPV4, additionally through direct association (Chen et al., 2017; Guo et al., 2017; Deng et al., 2018). This implies that VSLDs could affect channel gating (the process by which the pore opens or closes) upon interacting with chemical ligands. Beyond this relatively conserved transmembrane core, each TRP channel subtype is defined by a collection of unique soluble domains that may contribute to channel assembly and trafficking, and/or serve as receptor sites for numerous endogenous cellular factors or exogenous ligands.

Here, I review the wealth of recent structural data on TRP channels that have resulted largely from the “resolution revolution” in cryo-EM, with a particular focus on the conserved transmembrane core. I also discuss how these structures have enriched our understanding of function, regulation, and pharmacology of TRP channels. I apologize for any omissions of literature, due to the page limit and scope of this review.

The “resolution revolution” led to breakthrough in TRPV1 structural biology

Cryo-EM was arguably born in early 1980s when Dubochet and his colleagues invented a practical sample preparation method that affords rapid freezing of biological specimens within a thin layer of vitreous ice (Lepault et al., 1983; Adrian et al., 1984). This

breakthrough preserves fragile biological molecules in a frozen, hydrated native-like state, which not only ameliorates electron radiation damage but also protects the embedded biological samples from evaporation in high vacuum of a typical electron microscope. In earlier applications, cryo-EM has been impactful in elucidating structures of large biological assemblies (e.g., ribosomes and viruses) and, in some favorable cases, yielded near atomic structures for large and symmetric icosahedral viruses (Agrawal and Frank, 1999; Zhang et al., 2010; Grigorieff and Harrison, 2011). However, most cryo-EM reconstructions typically show densities of blobs only useful for demarcating distinct domains of a protein or identifying individual subunits in a multimeric complex, but insufficient to resolve secondary structures, letting alone side-chains of individual residues. Nevertheless, based purely on theoretical considerations, Richard Henderson and others presciently predicted that single-particle cryo-EM should be able to resolve structures of biological molecules as small as 100 kD at 3 Å or better resolutions in the 1990s, when cryo-EM was considered as a fringe technique and often referred to as “blobology” by x-ray crystallographers (Saxton and Frank, 1977; Henderson, 1995). Indeed, no one could foresee that, two decades later and around the end of 2012, steady advancements in electron microscopes, cameras, and computational algorithms finally reached a “tipping point” and, it appeared to many outsiders, have magically transformed the cryo-EM field overnight, leading to the so-called “resolution revolution” that is rapidly reshaping the landscape of structural biology (Kühlbrandt, 2014; Callaway, 2015). Application of a new generation of direct electron detectors (DEDs) has arguably contributed the lion’s share to this

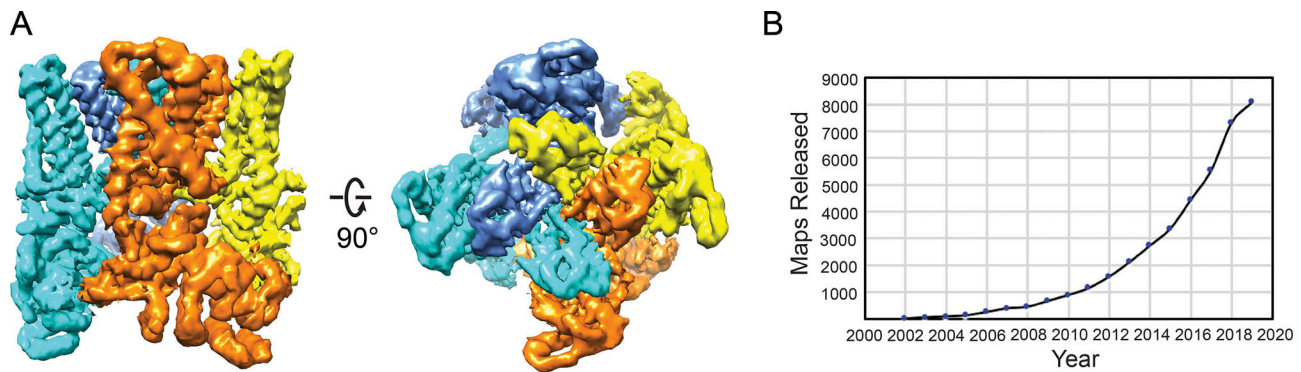


Figure 2. **Determination of TRPV1 structures by single-particle cryo-EM.** (A) The 3.4 Å map of TRPV1 determined by single-particle cryo-EM is shown in a side view (left) and a cytoplasmic view (right). (B) The “resolution revolution” in cryo-EM has led to a recent explosion of structures deposited at EMDB. The plot is available at https://www.ebi.ac.uk/pdbe/emdb/statistics_main.html/.

quantum leap in cryo-EM (Campbell et al., 2012; Li et al., 2013; McMullan et al., 2014, 2016). DEDs exhibit drastically improved detective quantum efficiency (a commonly used metric for quantifying camera performance) across all spatial frequencies. DEDs are now routinely employed to record much sharper micrographs with signals potentially extending to the maximum resolution limit of Nyquist frequency that can then be extracted to determine high-resolution structures using various computational algorithms (Frank et al., 1996; Grigorieff, 2007; Tang et al., 2007; Scheres, 2012; Punjani et al., 2017).

The emergence of the first high-resolution TRP channel structures coincided with the “resolution revolution” in cryo-EM (Fig. 2). TRPV1, the heat- and capsaicin-activated cation channel, was also the first integral membrane protein whose structure was determined at near atomic resolution by single-particle cryo-EM (Cao et al., 2013; Liao et al., 2013). On the technical front, these TRPV1 structures broke the side-chain resolution barrier for a membrane protein without crystallization for the first time. The Julius laboratory actually attempted to determine TRPV1 structures by x-ray crystallography in collaboration with Bob Stroud’s group at the University of California, San Francisco (San Francisco, CA). We, a team including Julio Cordero-Morales (now at the University of Tennessee Health Science Center, Memphis, TN), Thomas Tomasiak (now at the University of Arizona, Tucson, AZ), and me, obtained TRPV1 crystals growing in bicelles around early 2012, but unfortunately, these crystals only diffracted to 6–7 Å and were inadequate for structure determination despite extensive optimization efforts. More recently, crystal structures of TRPV6, TRPV2, and TRPV4 were reported (Saotome et al., 2016; Deng et al., 2018; Singh et al., 2018c; Zubcevic et al., 2018b), showcasing the strength of x-ray diffraction (even at modest resolutions) in unambiguously locating ions or small molecule modulators by exploiting their anomalous signals at special x-ray wavelengths.

The breakthrough in determining TRPV1 structures also exemplified how technical innovations can often spur discoveries in science. Indeed, single-particle cryo-EM is increasingly becoming the method of choice for resolving structures of membrane proteins and large protein complexes because these

targets are notoriously difficult to crystallize. On a side note, the growing popularity of cryo-EM in the structural biology community also highlights the urgent need to establish new and to support existing national cryo-EM centers where investigators without access to expensive and technically demanding high-end electron microscopes in their home institutions can still routinely collect data for determining structures of their favorite molecules (Stuart et al., 2016).

Ion selectivity filter of TRP channels

Most TRP channels are nonselective cation channels that conduct both monovalent and divalent cations (e.g., K^+ , Na^+ , and Ca^{2+}), with several notable exceptions: TRPV5 and TRPV6 are Ca^{2+} -selective channels in epithelia (Vennekens et al., 2000; Nilius et al., 2001; Yue et al., 2001), whereas TRPM4 and TRPM5 are only permeable to monovalent cations (Launay et al., 2002; Hofmann et al., 2003; Liu and Liman, 2003; Prawitt et al., 2003). Historically, the landmark KcsA structures were instrumental for us to understand the origin of K^+ selectivity (Doyle et al., 1998; Zhou et al., 2001b). These KcsA structures elegantly showed that K^+ selectivity could stem from a size-restrictive selectivity filter where backbone carbonyl oxygen atoms line the pore in a geometry optimal for coordinating the dehydrated K^+ ions but perhaps not the smaller Na^+ ions (Fig. 3). However, later molecular dynamic studies showed that the selectivity filter of K^+ channels is flexible and thus cannot discriminate K^+ over Na^+ solely based on their size difference of 0.38 Å, but nonetheless remains optimal for K^+ due to electrostatic properties of carbonyl oxygen ligands (Noskov et al., 2004). Regardless of the precise mechanisms of K^+ selectivity, all K^+ ion channels bear a signature selectivity filter sequence (i.e., TVGYG), which folds into almost identical 3-D structures that dictate K^+ selectivity of these channels (Kuang et al., 2015). For most TRP channels, however, no such recognizable unifying selectivity filter sequence or structural characteristics stands out to adequately explain how ion selectivity (or lack thereof) is achieved. TRP channel selectivity filters are not only diverse in size, ranging from 3.2 to 10.6 Å in diameter, but also lined with divergent amino acid sequences, albeit with aspartic acid and glycine residues commonly found. However, none of

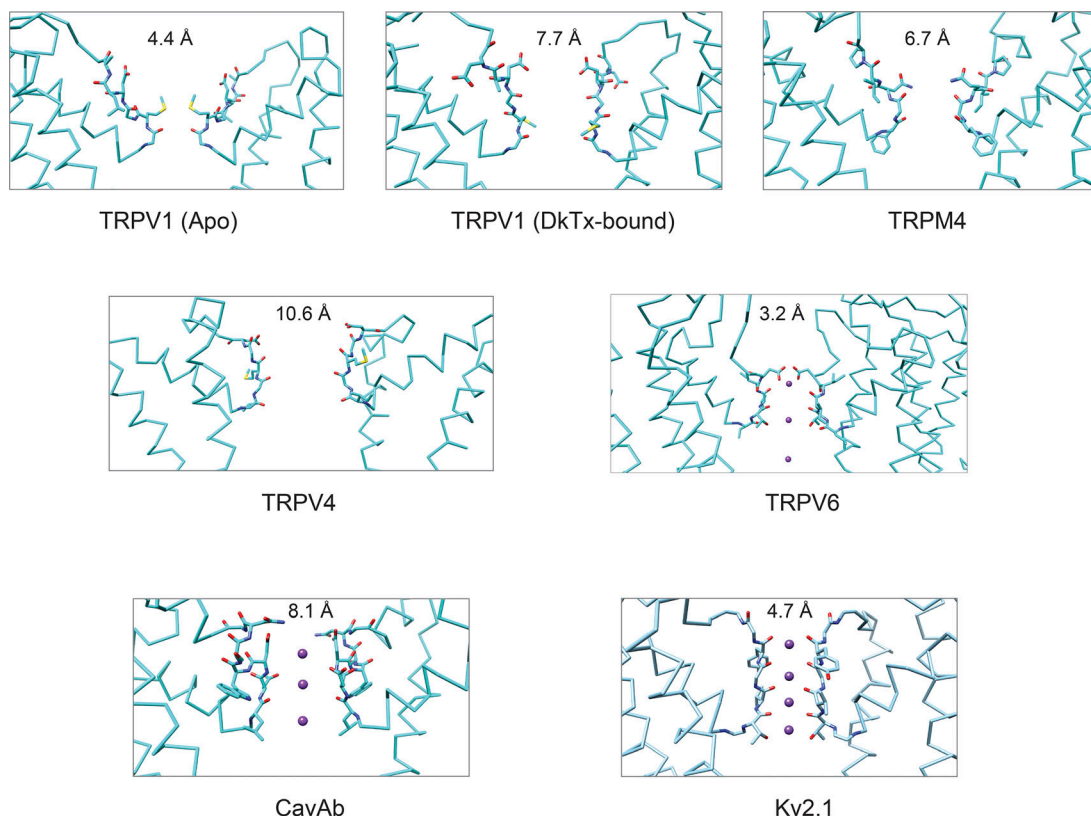


Figure 3. **Chemistry and size of the selectivity filter of representative TRP channels and VGICs.** TRP channel selectivity filters are diverse in both size and constituent residues. The diameters measured from two narrowest diagonally opposed oxygen atoms are shown at the top. The selectivity filters of Ca²⁺-selective CavAb and K⁺-selective Kv2.1 are also shown for comparison. Ions in TRPV6 (Ba²⁺), CavAb (Ca²⁺), and Kv2.1 (K⁺) are shown as purple spheres. PDB accession nos. are as follows: TRPV1-Apo (3J5P), TRPV1-DkTx (3J5R), TRPM4 (6BQR), TRPV4 (6BBJ), TRPV6 (5IWR), CavAb (5KLB), and Kv2.1 (2R9R).

these features can reliably predict the level of selectivity to various cations (Fig. 3). Ion selectivity of TRP channels is perhaps defined by interaction energy of competing permeable cations with dynamic selectivity filters, which is beyond what can be gleaned from only inspecting the existing static snapshots of TRP channel structures. Further experiments, such as molecular dynamic studies performed for TRPV1 (Jorgensen et al., 2016) and TRPV6 (Sakipov et al., 2018), are needed to fill this gap of knowledge. Nevertheless, as discussed below, the selectivity filters of TRP channels do conform to the same basic design principles that have emerged from structural analyses of K⁺ (Doyle et al., 1998), Na_v (Payandeh et al., 2011; Zhang et al., 2012; Shen et al., 2017; Yan et al., 2017; Pan et al., 2018; Jiang et al., 2019), and Ca_v channels (Tang et al., 2014; Wu et al., 2016). These principles are expected to be generally applicable to other cation-selective ion channels as well.

First, the selectivity filter of TRP channels is cradled by one (in all TRPV channels) or two pore helices (perhaps in all other TRP channels). At the outermost site of their selectivity filter facing the extracellular vestibule, most TRP channels harbor a negatively charged residue, predominantly aspartic acid (Fig. 3). Four Asp residues (DDDD), one from each subunit, form a negatively charged ring, offering an immediate impression that they are strategically positioned to either attract and/or directly coordinate cations; these Asp residues could also repel anions from

the filter. Neutralization of this negative charge affects ion selectivity of many TRP channels, including TRPV1 (Chung et al., 2008), TRPV4 (Voets et al., 2002), TRPV5 (Nilius et al., 2001), TRPV6 (Voets et al., 2004b), TRPM7 (Duan et al., 2018b), fly TRP channels (Liu et al., 2007), TRPA1 (Christensen et al., 2016), and PKD2L1 (Fujimoto et al., 2011; DeCaen et al., 2016). TRPM4 and human TRPM2 (Guo et al., 2017; Winkler et al., 2017; Autzen et al., 2018; Duan et al., 2018c), but not *Nematostella vectensis* TRPM2 (Zhang et al., 2018b), are notable exceptions in having a glutamine at the outermost position of their selectivity filters (Fig. 3), which appears to underlie their lack of permeability to divalent cations (e.g., Mg²⁺ and Ca²⁺). Indeed, substitution of this glutamine to glutamate in TRPM4 restores negative charges in the selectivity filter and confers moderate Ca²⁺ permeability (Nilius et al., 2005). Such a design principle is evolutionarily ancient, as an analogous structure (EEEE) is also present in bacterial homotetrameric Na_v and Ca_v (Ren et al., 2001; Zhang et al., 2012; Tang et al., 2014). In some eukaryotic Na_v and Ca_v, however, a lysine residue replaces the Asp/Glu at the second or third position, giving rise to alternative EKEE or EEKE arrangements (Stephens et al., 2015). Notwithstanding variations to this basic negatively charged ring structure, the conserved Asp or Glu, found in both VGICs and TRP channels, likely serves as the high-field-strength site predicted by Hille decades before atomic structures of VGICs and TRP channels were resolved (Hille, 1971, 1972).

Second, as observed in KcsA and VGICs, backbone carbonyl oxygen atoms of some selectivity filter residues also face the pore in TRP channels, possibly forming additional coordination sites for cations (Fig. 3). In some cryo-EM maps of TRP channels, non-protein densities were indeed observed within the selectivity filter and thus interpreted to represent permeating cations (Chen et al., 2017; Guo et al., 2017; Hirschi et al., 2017; Wilkes et al., 2017; Duan et al., 2018b,c; Hughes et al., 2018a; Zhang et al., 2018b). In TRPV6 and TRPV4 crystal structures, the ion coordination sites were unambiguously confirmed by exploiting anomalous signals of more electron dense ions, such as Cs^+ , Gd^{3+} , and Ba^{2+} (Saotome et al., 2016; Deng et al., 2018). Multiple closely spaced ion binding sites were initially observed in KcsA crystal structures (Doyle et al., 1998), and later in voltage-gated Na^+ and Ca^{2+} as well (Payandeh et al., 2011; Tang et al., 2014), an arrangement that appears to support a “knock-off” mechanism whereby repulsion between adjacent ions would overcome the attractive interactions between ions and the channel protein so as to achieve rapid rates of ion conduction that, in some cases, can approach the diffusion limit (Almers and McCleskey, 1984; Hess and Tsien, 1984; Neyton and Miller, 1988). As might have been expected from their close kinship to VGICs, many TRP channels also likely consist of multiple ion binding sites within the selectivity filter, indicating that such a “knock-off” mechanism of ion permeation may also be pervasive in the TRP channel superfamily (Jorgensen et al., 2016; Saotome et al., 2016; Sakipov et al., 2018). Surprisingly, only a single ion-binding site was identified in the current TRPV4 crystal structures (Deng et al., 2018). TRPV4 also boasts the widest selectivity filter (~10.6 Å in diameter; Fig. 3) among all TRP channels for which structures have been determined, implying that fully hydrated cations could diffuse freely through the filter and probably only interact very weakly with the pore lining residues. Such a wide selectivity filter might explain the unusually large single channel conductance of TRPV4 (~280–310 pS) when Ca^{2+} is included as a charge carrier (Liedtke et al., 2000). Of note, in a Ca^{2+} -free condition, single-channel conductance of TRPV4 reduces to ~100 pS, which is comparable to the related TRPV1 channel (Hui et al., 2003). Therefore, it remains to be determined whether TRPV4 contains multiple ion binding sites in other conformational states as do most other TRP channels, or it utilizes a distinct permeation mechanism based on a single ion binding site.

Finally, in some TRP channels, the selectivity filter may function as a gate (or upper gate), in addition to the more common gate (or lower gate) formed by hydrophobic residues located near the cytoplasmic end of the pore lining S6 helix. TRPV1 was speculated to harbor an upper gate based on the observations that a pore helix mutation leads to a constitutively open channel and that spider toxins (e.g., double knot toxin [DkTx]) activate TRPV1 by binding to and stabilizing the outer pore region in an open conformation (Myers et al., 2008; Bohlen et al., 2010). In addition, state-dependent accessibility of substituted cysteine residues along the S6 helix predicted that two constrictions exist in the TRPV1 ion permeation pathway (Salazar et al., 2009). Indeed, TRPV1 structures captured in three distinct pore conformations, presumably representing apo-closed, capsaicin-bound partially open, and resiniferatoxin

(RTX)- and DkTx-bound open states (Cao et al., 2013; Gao et al., 2016), show gating-associated structural changes within the selectivity filter region. Comparison of these structures shows that, upon binding DkTx, the narrowest constriction of the selectivity filter expands from 4.4 to 7.7 Å (Fig. 3). DkTx binding evokes two salient structural changes within the selectivity filter region: first, a methionine in the middle of the selectivity filter rotates so that its side chain no longer points toward the center of the pore to obstruct ion permeation as observed in the apo state; second, four Asp residues, one from each subunit, residing at the extracellular mouth of the selectivity filter, moving toward the central axis of the pore, as if they are now better positioned to coordinate and partially dehydrate cations for efficient ion conduction. In a TRPV2 channel engineered to be sensitive to RTX, an even more drastic dilation of the upper gate was recently observed as the channel transitions from fourfold to twofold symmetry upon binding RTX (Zubcevic et al., 2018b), further confirming the existence of an upper gate within the TRPV channels. Such flexibility within the TRPV1 outer pore region also likely contributes to distinct single-channel conductance states evoked by different TRPV1 agonists (Canul-Sánchez et al., 2018; Geron et al., 2018).

However, one potential caveat of these structural analyses is how faithfully these TRPV structures resemble channel conformations in native cells. For instance, a recent study showed that the selectivity filters of TRPV1–3 channels are permeable to Ag^+ ions even in a closed state and thus possibly do not gate permeation of physiological cations (Jara-Oseguera et al., 2019). Irrespective of whether TRPV1 harbors a selectivity filter gate, its dynamic outer pore region and potential allosteric communications with the lower conventional activation gate undoubtedly contribute to its complex regulation by endogenous ligands and a wide range of pharmacological compounds.

In most non-TRPV TRP channels, the selectivity filter is rigidly framed between two pore helices as observed in VGICs, making conformation changes within the selectivity filter region unlikely, if not impossible. Indeed, in the agonist ML-SA1-bound structures of TRPML1 and TRPML3 channels, the selectivity filter region only shows negligible changes as compared with the apo state, if there are any, whereas the lower gate undergoes significant expansion (Schmiege et al., 2017; Zhou et al., 2017). Similarly, TRPM2 also shows no conformational changes in the selectivity filter region when comparing TRPM2 structures determined in presumably closed, sensitized (i.e., primed for activation), or open states (Wang et al., 2018). Moreover, in TRPV5 and TRPV6 channels, the selectivity filter also remains stationary during channel gating (Hughes et al., 2018b; McGoldrick et al., 2018; Singh et al., 2018b,c; Dang et al., 2019), as might have been anticipated for a Ca^{2+} -selective channel since a dynamic selectivity filter would be counterproductive for maintaining an optimal geometry essential for strict Ca^{2+} -selectivity. Finally, a much wider selectivity filter, comparable in size to that observed in the DkTx-bound TRPV1 structure, exists in many TRP channels determined presumably in closed states (Fig. 3), implying that, in these channels, only the lower gate controls ion permeation, whereas the selectivity filter may be always permissive to ion conduction. Of course, we should be cautious not

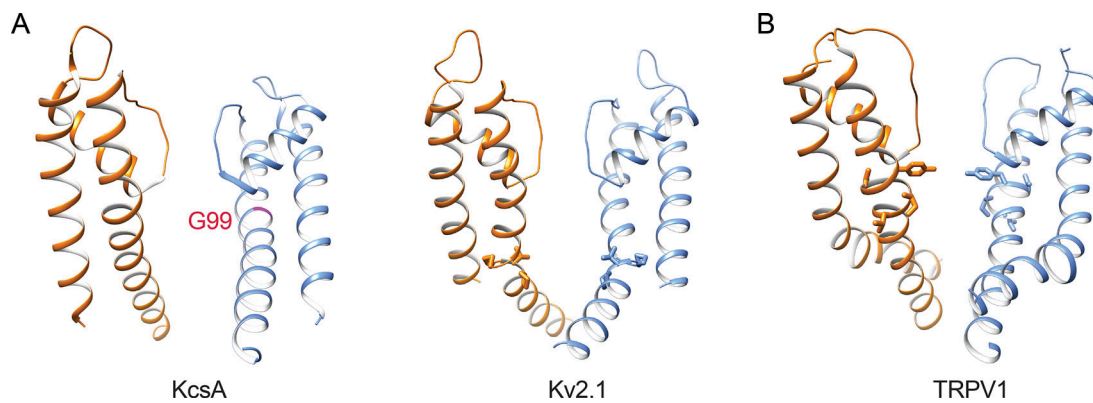


Figure 4. **Structural elements that confer conformational flexibility to the pore lining S6 helix in K⁺ and TRPV1 channels.** (A) Gating hinges in KcsA (Gly99; red) and Kv2.1 (Pro-Val-Pro; shown in sticks) allow for splaying open of their activation gates. (B) A π -helix bulge, highlighted in sticks, likely provides a flexing point around which the distal S6 helix can rotate and/or bend to open the lower gate in TRPV1. PDB accession nos. are as follows: KcsA (5VKF), Kv2.1 (2R9R), and TRPV1 (3J5R).

to overinterpret these structural data as they may not capture all conformational states that a TRP channel can sample as it progresses along its gating cycle on native cells. Indeed, TRPV5, a close homologue of TRPV6, is inhibited by acidification, possibly due to proton-induced conformational changes in the pore helix (Yeh et al., 2005).

The hydrophobic lower gate

In all TRP channels whose structures have been determined so far, hydrophobic residues, residing near the intracellular end of the pore lining S6 helices, point their side chains toward the center of the pore, forming a hydrophobic seal (or lower gate) that blocks ion permeation. In K_v channels, the S6 helix contains a -Pro-X-Pro- motif and/or a glycine residue, located roughly at the middle of the lipid bilayer (Jiang et al., 2002; Long et al., 2005a). These so-called gating hinge elements can function independently or in tandem to permit splaying open of the lower half of the S6 helix upon activation induced by membrane depolarization (Labro and Snyders, 2012). TRP channels appear to lack such a gating hinge, but instead harbor a conserved π -helix at a similar position (Fig. 4). Compared with canonical α -helices, π -helices are high-energy and conformationally dynamic secondary structures often found in functional sites of proteins (Cooley et al., 2010). The S6 π -helix was first speculated to play a role in TRP channel gating based on comparative sequence analysis (Palovcak et al., 2015). Later, by comparing TRPV2 and TRPV1 structures, transition of this π -helix to a canonical α -helix was hypothesized to mediate TRPV2 gating (Zubcevic et al., 2016). More recently, it was directly shown that an α - to π -helix transition opens the lower gate of TRPV6 (McGoldrick et al., 2018). Such a transition from a low- to high-energy state, on the surface, is counterintuitive, but it can be rationalized that the high-energy π -helix is compensated by formation of new hydrophilic interactions within its neighboring regions (McGoldrick et al., 2018). Similarly, an α - to π -helix transition in S6 accompanies the transition from a closed to sensitized or open state in TRPV3 (Singh et al., 2018a; Zubcevic et al., 2018a, 2019), and from a closed to desensitized state in TRPM8 (Diver et al., 2019). We found that a gain-of-function (F604P) mutation

in PKD2 leads to an opposite π - to α -helix transition, resulting in dilation of the lower gate that might underlie constitutive channel activity of this mutant (Arif Pavel et al., 2016; Zheng et al., 2018). In the TRPV1 channel, however, the π -helix structure maintains regardless of pore conformations (Cao et al., 2013). Nevertheless, it is interesting to note that the π -helix is precisely the point below which the distal S6 segment starts to diverge when superimposing structures of the pore captured in three distinct states, thus functionally analogous to the gating hinge in K_v channels.

In TRPML1 and TRPML3 channels, the S6 π -helix appears to play no role in agonist (ML-SA1)-induced channel activation (Schmiege et al., 2017; Zhou et al., 2017). ML-SA1 binds to a hydrophobic pocket located above the π -helix, leading to outward movement of the entire S6 helix, and consequently, expansion of the lower gate. However, it remains to be determined whether other stimuli, such as phosphoinositides in combination with membrane depolarization, open the TRPML channels by facilitating structural transition of the S6 π -helix. Similarly, in TRPM2, adenosine diphosphate ribose (ADPR) and Ca²⁺ together trigger dilation of the lower gate, which appears to not involve the S6 π -helix (Huang et al., 2018; Wang et al., 2018). Notably, the S6 π -helix has not been identified in structures of PKD2L1 channels (Hulse et al., 2018; Su et al., 2018b), and future studies will determine whether the π -helix exists in other states of this channel. Taken together, unlike the upper selectivity filter gate, the lower gate is present in all TRP channels, and the prevalent S6 π -helix may act as a dynamic flexing point around which the distal S6 segment can rotate and/or bend to open the lower gate (Zubcevic and Lee, 2019).

The VSLD

The classic voltage-sensor domain (VSD) consists of four helices (S1–S4) and plays a predominant role during gating of VGICs (Catterall, 1986, 2010; Aggarwal and MacKinnon, 1996; Long et al., 2005a; Bezanilla, 2018). In particular, the S4 helix bears an array of four to six positively charged arginine or lysine residues (or gating charges) at every fourth position that are stabilized in an otherwise inhospitable hydrophobic and low

dielectric lipid bilayer by negatively charged residues protruding from other helices (Long et al., 2007; Payandeh et al., 2011). These residues form two charge clusters separated by a highly conserved phenylalanine residue. Channel gating elicited by changes in membrane potential is believed to involve transfer of positively charged residues from the external charge cluster, across this phenylalanine gap, to the internal charge cluster, or vice versa (Tao et al., 2010; Vargas et al., 2012; Li et al., 2014). Such large motion of the S4 helix is believed to exert force on the S4–S5 linker, leading to its outward or inward movement with respect to the pore domain that ultimately opens or closes the activation gate of VGICs.

In contrast to VGICs, most TRP channels only exhibit weak voltage sensitivity generally manifested as an outwardly rectifying I–V relationship in electrophysiological recordings (Wu et al., 2010), as if membrane depolarization promotes channel opening and/or sensitizes channel to other stimuli (Brauchi et al., 2004; Voets et al., 2004a). The VSLD of TRP channels lacks most, if not all, of the positively charged residues along the S4 helix, providing a simple explanation for their weak voltage sensitivity as compared with VGICs. For instance, TRPV1 and TRPM8 show apparent gating charges of less than 1 e as compared with 13 e measured for the Shaker K⁺ channel (Schoppa et al., 1992; Voets et al., 2004a; Matta and Ahern, 2007). PKD2L1 represents a notable exception as it retains two gating charges, and channel activation by disparate stimuli all requires transfer of a total of approximately four gating charges (i.e., a single gating charge per subunit; Ng et al., 2019). Nevertheless, the VSLD of most TRP channels, as first observed in TRPV1 (Cao et al., 2013), is rigid and remains static during channel gating. For instance, the VSLD was also shown to remain relatively stationary in TRPV6 (McGoldrick et al., 2018), PKD2 (Shen et al., 2016; Grieben et al., 2017; Wilkes et al., 2017; Zheng et al., 2018), TRPML1 (Schmiege et al., 2017), TRPM2 (Huang et al., 2018; Wang et al., 2018), TRPV2 (Dosey et al., 2019), TRPV3 (Singh et al., 2018a), and TRPML3 channels (Zhou et al., 2017), for which structures captured in presumably open and closed states have been determined to discern mobile structural elements during channel gating. More recently, the VSLD of TRPA1 was shown to undergo a rigid body rotation relative to the pore domain upon activation by cystine reactive irritants (Zhao et al., 2019), highlighting a vast conformational landscape accessible to polymodal TRP channels.

In addition to a lack of gating charges along the S4 helix, the VSLD of TRP channels often associates extensively with the pore domain, in sharp contrast to K_v channels, where only minimal contacts exist at a small extracellular interface between the S1 helix of one subunit and the S5 helix from a neighboring subunit (Fig. 5; Long et al., 2005a). Generally speaking, in VGICs, VSD appears to be largely indirectly coupled to the pore domain via the S4–S5 linker, and the voltage-sensing S4 helix is “free” to move relative to the pore domain. In the Shaker K_v channel, direct interactions between the VSD and pore domain additionally contribute to electromechanical coupling (Soler-Llavina et al., 2006; Fernández-Mariño et al., 2018). In TRPM4 and TRPML1, however, the S4 helix exhibits extensive hydrophobic interactions with the S5 helix from an adjacent subunit for

virtually its entire length, making large translational movement of the S4 helix unlikely in these channels (Fig. 5; Chen et al., 2017; Guo et al., 2017). In TRPV4, the VSLD engages with the pore domain via an even more extensive interface involving the S3 and S4 helices of one subunit and the S5 and S6 helices of a neighboring subunit (Fig. 5; Deng et al., 2018). Additionally, the S3 helix of TRPV4 appears to be directly coupled to the pore lining S6 helix, suggesting that it could transduce stimuli acting on the VSLD to impact the S6 activation gate by exerting force on the S6 helix (Deng et al., 2018).

TRP channels and VGICs differ significantly in structures of their S1–S4 domains, which undoubtedly contributes to their fundamentally distinct gating mechanisms. Nevertheless, the last two or three turns of the S4 helix of TRP channel often adopts a ₃₁₀-helical fold, as observed in VGICs. Similar to π -helix, ₃₁₀-helix is also highly energetic and conformationally dynamic (Enkhbayar et al., 2006; Vieira-Pires and Morais-Cabral, 2010). Indeed, subtle conformational changes within the ₃₁₀-helix have been observed in TRPV1 (Gao et al., 2016), TRPV6 (McGoldrick et al., 2018; Singh et al., 2018b,c), and PKD2 (Zheng et al., 2018) to cause and/or accommodate gating-associated structural rearrangements in the S4–S5 linker and TRP helix.

Ligand and lipid binding sites

TRP channels are versatile cellular sensors for a wide range of physiological and environmental signals, and elucidating how these channels interact with and respond to chemical ligands and physical stimuli is of paramount importance for understanding unique aspects of TRP channel pharmacology, regulation, and function. As would have been anticipated for polymodal sensory ion channels, each TRP channel often harbors multiple receptor sites that are exploited by small chemical compounds, peptide toxins, or cellular factors to regulate channel function. Here, I highlight major regulatory sites emerged from structural analyses of TRP channels.

The vanilloid binding pocket. TRPV1 was first cloned in 1997 by the Julius group, as expression of this channel confers sensitivity to the pungent vanilloid compound capsaicin to otherwise capsaicin-insensitive HEK293 host cells (Caterina et al., 1997). Birds, however, are spared of the “burning” effects of capsaicin, and indeed, capsaicin acts as a partial agonist for chicken TRPV1 (Jordt and Julius, 2002). By exploiting this natural difference in capsaicin sensitivity, chimeras of rat and chicken TRPV1 were constructed to delimit the vanilloid-binding site to a minimal region encompassing the S2 and S3 helices, including Y511, which was hypothesized to directly engage the vanilloid moiety of capsaicin molecule (Jordt and Julius, 2002). Further mutagenesis studies also pinpointed residues on the S4 helix for specifying sensitivity to various vanilloid ligands (Chou et al., 2004; Gavva et al., 2004; Phillips et al., 2004). It is gratifying that TRPV1 structures bound with capsaicin, RTX, or capsazepine (a TRPV1 antagonist) are in excellent agreement with these mutagenesis studies. These structures showed that all these vanilloid ligands are buried within a pocket formed by S3, S4, and the S4–S5 linker from one subunit and the pore domain (i.e., S5 and S6 helices) of an adjacent subunit (Cao et al., 2013;

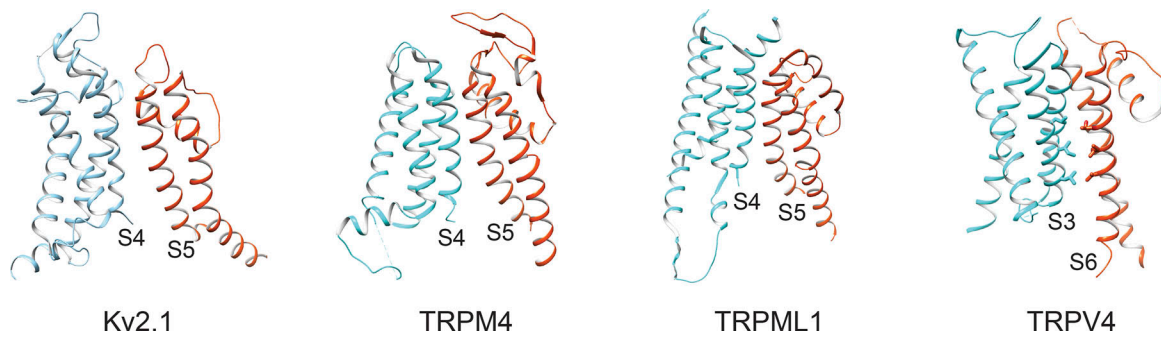


Figure 5. **Association of the S1–S4 domain with the pore domain in representative TRP and K_v channels.** TRP channel voltage-sensor like domain (VSLD; cyan) typically associates with pore domain from an adjacent subunit (orange; red) via a larger interface and thus remains relatively static during channel gating as compared with VGICs. The potential hydrophobic interactions between the S3 and S6 helices in TRPV4 are highlighted with sticks. PDB accession nos. are as follows: Kv2.1 (2R9R), TRPM4 (6BQR), TRPML1 (5WJ5), and TRPV4 (6BBJ).

Gao et al., 2016). The Y511 residue indeed plays a prominent role in binding vanilloid compounds, as its aromatic ring is induced to point toward the pocket to engage ligands, as opposed to facing cytosol in apo state. Vanilloid agonists, such as RTX and capsaicin, appear to directly interact with and pull the S4–S5 linker away from the central pore, and consequently facilitate opening of the lower gate (Yang et al., 2015a; Gao et al., 2016).

Remarkably, a mere introduction of four to six point mutations into TRPV2 or TRPV3 so as to mimic the TRPV1 vanilloid site confers RTX sensitivity to the otherwise insensitive channels, further validating the vanilloid binding pocket defined by structures and computational studies (Yang et al., 2016; Zhang et al., 2016, 2019). More broadly, the vanilloid pocket also represents the site of action of other small molecule modulators for other TRP channels, including a TRPC6 antagonist BTDM and a TRPV5 antagonist econazole (Hughes et al., 2018a; Tang et al., 2018).

Intriguingly, the vanilloid pocket harbors a resident lipid, perhaps phosphoinositides, in apo state. Vanilloid ligands were therefore hypothesized to displace this lipid to produce either agonistic or antagonistic effects (Gao et al., 2016). However, it was also shown that a cytoplasmic arginine residue distant from the vanilloid pocket specifies sensitivity of TRPV1 to different phosphoinositide species, suggesting that multiple phosphoinositide binding sites may exist in TRPV1 (Ufret-Vincenty et al., 2015).

A regulatory site at the cytoplasmic opening of VSLD. In VGICs, VSD is frequently targeted from the extracellular side by a large class of gating modifier toxins found in animal venoms, reinforcing the notion that movement of VSD is fundamental for gating these channels (Alabi et al., 2007; Catterall et al., 2007; Bosmans et al., 2008; Kalia et al., 2015). In contrast, in most TRP channels, the equivalent VSLD and its constituent S4 helix appear to remain relatively stationary during channel gating, and so far, peptide toxins were only identified to bind to the presumably more dynamic outer pore region of TRPV1 (Kitaguchi and Swartz, 2005; Cuyper et al., 2006; Siemens et al., 2006; Andreev et al., 2008; Bohlen et al., 2010; Yang et al., 2015b). Nevertheless, the S4–S5 linker, which relays movements of VSD to the pore in VGICs, is similarly positioned to affect the lower gate in TRP channels. Therefore, the S4–S5 linker in TRP

channels can transduce subtle conformational changes induced by ligands acting on the VSLD to allosterically gate the pore. Indeed, in TRPV6, antagonist 2-APB binds to a cytoplasmic opening of VSLD, causing the S3 helix to move toward the S4–S5 linker; such subtle structural rearrangements foster formation of a hydrophobic cluster composed of residues from the S2–S3 linker, the cytoplasmic end of the S3 and S4 helices, and the S4–S5 linker, which in turn appears to disengage a presumably activating lipids from the S4–S5 linker and ultimately closes the channel pore (Singh et al., 2018c). Similarly, an antagonist of TRPV5 identified by in silico docking screen binds to an analogous site and inhibits channel activation (Hughes et al., 2019). In TRPM2, TRPM4, TRPM8, and TRPA1 structures, a Ca^{2+} ion is coordinated by hydrophilic residues at an equivalent site (Guo et al., 2017; Winkler et al., 2017; Autzen et al., 2018; Duan et al., 2018c; Huang et al., 2018; Wang et al., 2018; Yin et al., 2018; Zhang et al., 2018b; Yin et al., 2019a,b; Zhao et al., 2019); this Ca^{2+} -binding site is essential for activation of TRPM8 by a cooling compound icilin, as well as for activation and desensitization of TRPA1 downstream of metabotropic receptors (Yin et al., 2019a; Zhao et al., 2019). In TRPM8, this pocket appears to be malleable to also accommodate both antagonists and agonists of diverse chemical structures (Diver et al., 2019; Yin et al., 2019a). Moreover, in TRPC4, a non-protein density at a similar hydrophilic pocket was tentatively modeled as a Na^+ ion, the predominant ion in the specimen used for structure determination (Duan et al., 2018a). Taken together, many TRP channels have evolved a pocket of distinct chemical properties (i.e., hydrophobic or hydrophilic) on the cytoplasmic side of VSLD to accommodate various ligands such as 2-APB, icilin, menthol, or ions that can allosterically regulate channel gating.

The outer pore region. The outer pore region of several TRPV channels is known to be involved in activation by chemical ligands (Jordt et al., 2000; Yeh et al., 2005; Ryu et al., 2007). For instance, two glutamate residues located at the outer pore region of TRPV1 are essential for acid-evoked potentiation or activation (Jordt et al., 2000). The outer pore region similarly serves as a receptor site for environmental or physiological stimuli in other TRP channels. For example, in both TRPC4 and TRPC5, a disulfide bond in the outer pore region confers redox-sensitivity as application of reducing reagents (e.g., dithiothreitol or TCEP)

potentiates channel currents (Xu et al., 2008; Hong et al., 2015; Duan et al., 2018a; Vinayagam et al., 2018). An analogous disulfide bond exists in several members of the TRPM subfamily, but whether it also regulates channel activity remains unclear. Finally, just as plants have evolved pungent TRPV1-activating vanilloid compounds (e.g., capsaicin and RTX) to discourage herbivory, venomous animals, such as spiders and centipedes, produce peptide toxins that agonize TRPV1 to elicit acute pain perhaps for predator deterrence (Siemens et al., 2006; Bohlen et al., 2010; Yang et al., 2015b). Remarkably, these peptide toxins, despite their distinct structural fold and different origin, all convergently target the TRPV1 outer pore region to exert their effects, unmistakably proving that the outer pore region serves as a critical allosteric site in TRPV1 and perhaps in other TRP channels as well.

The TRPV1 structures bound with DkTx spider toxin showed that the toxin inserts into a crevice formed by the outer pore region of two neighboring subunits (Fig. 6; Cao et al., 2013; Bae et al., 2016; Gao et al., 2016). Interestingly, several lipids were found to mediate interactions between DkTx and TRPV1, suggesting that lipids may modulate pharmacological effects of DkTx (Bae et al., 2016; Gao et al., 2016). This observation is consistent with the notion that some inhibitory cysteine knot toxins, to which DkTx belongs, first partition into the lipid bilayer, where they are believed to be concentrated and gain unobstructed access to receptor sites on channel protein via free lateral diffusion (Lee and MacKinnon, 2004). Of note, the DkTx toxin appears to stabilize the TRPV1 outer pore region in an open conformation without making discernable contacts with the VSLD, setting it apart from a large class of gating modifier toxins that target the VSD of VGICs. Generally speaking, voltage-sensor toxins principally latch onto VSD and perhaps are further constrained by anchoring to adjacent extracellular loops or lipid bilayer, thus physically impeding voltage sensor movement (Fig. 6; Shen et al., 2018, 2019; Xu et al., 2019). DkTx also differs significantly from pore blocking peptide toxins, such as charybotoxin and μ -conotoxin KIIIA, that insert a lysine into the entrance to selectivity filters and essentially plug the extracellular ion entryway of various K^+ and Na_v channels, respectively (Fig. 6; Banerjee et al., 2013; Pan et al., 2019).

Pockets near the pore helix. In TRPA1, a relatively occluded pocket surrounded by S5, S6, and pore helix 1 from a single subunit constitutes the receptor site for antagonist A-967079, which may act as a molecular wedge that inhibits activation-associated conformational changes (Paulsen et al., 2015). In TRPV2, agonist cannabidiol interacts with a topologically analogous pocket to promote channel opening (Pumroy et al., 2019). In TRPML1 and TRPML3, the ML-SA1 agonist binds to a lipid-facing cleft at the interface of pore modules, which is enclosed by pore helix 1, S5, and S6 from one subunit, and S6 of a neighboring subunit (Schmiege et al., 2017; Zhou et al., 2017). The ML-SA1-binding site likely harbors endogenous lipids in apo state, and ML-SA1 binding appears to squeeze out these resident lipids, pushes the S6 helix away from the central axis, and consequently expands the lower gate. Lipids play important structural and regulatory roles for membrane proteins, so it should not come as a surprise that many small molecule

compounds, including ivermectin (a partial inverse agonist of pentameric ligand-gated ion channels) and vanilloids (ligands of the TRPV1 channel), appear to compete with lipids for the same or overlapping binding sites to regulate ion channel activity (Hibbs and Gouaux, 2011; Cao et al., 2013; Gao et al., 2016). Notably, lipid-like densities are also observed in or near the ML-SA1-binding pocket in other TRP channels, including PKD2 and TRPC3 (Shen et al., 2016; Grieben et al., 2017; Wilkes et al., 2017; Fan et al., 2018), raising the possibility that this site could be similarly exploited to target these channels for drug discovery as well. More broadly, in related Ca_v channels, an equivalent pocket is the receptor site for dihydropyridines, a large class of Ca^{2+} antagonist drugs that are widely prescribed for treating cardiovascular disorders (Tang et al., 2016).

The cytoplasmic opening of the pore. Some TRP channels undergo Ca^{2+} -dependent inactivation and, in TRPV5 and TRPV6, this process is mediated through direct interaction with calmodulin (CaM; Nilius et al., 2003; Lambers et al., 2004). The recently reported structures of TRPV5 or TRPV6 bound with CaM showed that a lysine residue, located at the H6–H7 loop of CaM, inserts its side chain into the cytoplasmic entryway of channel pore, where it establishes cation- π interactions with a ring of four tryptophan residues (one from each subunit), leading to inward movement of the lower half of S6 helices, and consequently, pore closure (Hughes et al., 2018b; Singh et al., 2018b; Dang et al., 2019).

More broadly and beyond TRP channels, it has long been known that the ion permeation path of many ion channels bears receptor sites for small or medium-sized molecules. These include blocking ions (e.g., Gd^{3+}) that compete with permeating ions for binding sites within the selectivity filter, and small organic molecules that bind to other disparate sites along the pore (Voets et al., 2004b; Oseguera et al., 2007; Saotome et al., 2016). For instance, Shaker-type K^+ channels are blocked by tetrabutylammonium, a small organic cation (Armstrong, 1971). These channels also close spontaneously after opening induced by depolarization in an inactivation process whereby inactivation gate, a stretch of ~20 amino acids “ball peptide” from the N terminus of either α - or β -subunit of these channels, physically plugs the open pore from intracellular side (Hoshi et al., 1990; Zagotta et al., 1990; Rettig et al., 1994). Structural studies lately confirmed that pore opening provides a cytoplasmic entryway for tetrabutylammonium and “ball peptide” to gain access to central cavity sites below the selectivity filter and inner pore sites, ultimately leading to blockage of ion permeation (Zhou et al., 2001a). Moreover, Br-verapamil and flecainide, two drugs widely used for treating arrhythmias, respectively reach an analogous site in Ca_vAb and Nav1.5 via open pore and occlude the ion-conduction pathway (Tang et al., 2016; Jiang et al., 2019).

Regulatory sites within soluble domains. From a bird’s-eye view, most TRP channels are homotetramers, exhibiting fourfold symmetry around a central ion permeation pathway. There are several notable departures from this general architecture: structural analyses of TRPV2, TRPV3, and TRPM2 channels show that fourfold symmetry can be broken and reduced to twofold symmetry (Zubcevic et al., 2018a,b; Yin et al., 2019b), and the recently determined PKD1/PKD2

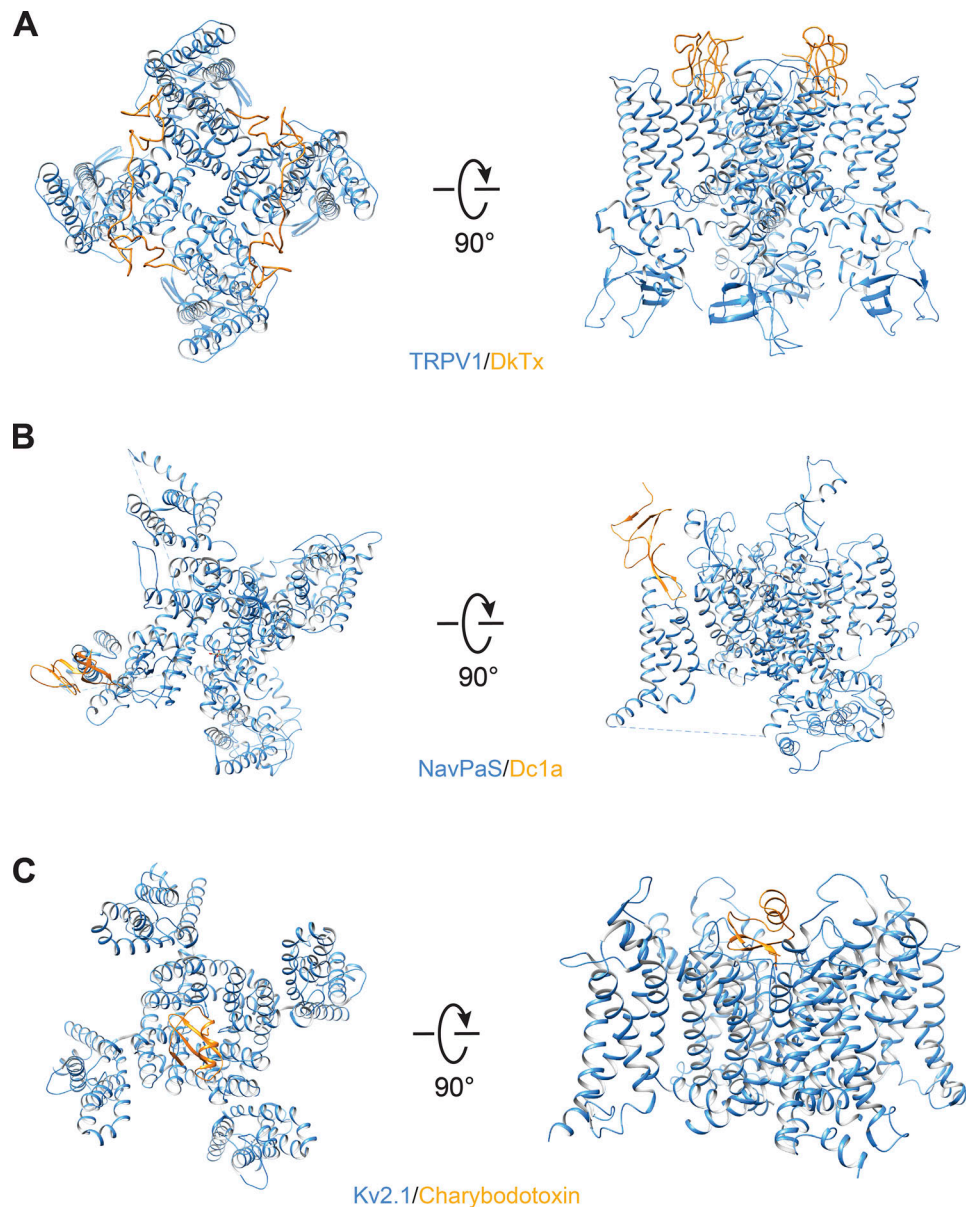


Figure 6. **Receptor sites for animal toxins targeting TRPV1 and VGICs.** (A) The spider DkTx toxin latches onto the outer pore region of TRPV1 and stabilizes an open pore conformation. (B) Dc1a wedges into a cleft between the VSD and pore domains of Na_v and impedes VSD movement. (C) Charybodotoxin inserts a lysine side chain into the extracellular entrance to the selectivity filter of K_v and physically plugs the entryway of ion permeation. PDB accession nos. are as follows: TRPV1/DkTx (5IRX), NavPaS (6A90), and $\text{K}_v2.1$ /charybodotoxin (4JTC).

structure, a heteromeric complex, understandably exhibits no symmetry at all (Su et al., 2018a). All TRP channels share a roughly similar transmembrane core composed of VSLD and pore domain, indicative of relatedness within this large cation channel family. However, outside the lipid bilayer, each TRP subtype consists of a combination of unique soluble domains located at both intracellular and extracellular sides. These widely diverse soluble domains can serve as receptor sites for numerous endogenous cellular factors or exogenous ligand(s) and thus undoubtedly contribute to unique aspects of function, regulation, and pharmacology of each TRP subfamily. TRP channel structures allow for direct visualization of some of these important regulatory sites located in these

soluble domains, including the IP_6 -binding site in TRPA1 (Paulsen et al., 2015), a reactive pocket targeted by electrophile irritants in TRPA1 (Suo et al., 2019; Zhao et al., 2019), ATP-binding sites in TRPM4 (Guo et al., 2017), ADPR binding site in TRPM2 (Huang et al., 2018; Wang et al., 2018; Yin et al., 2019b), and decavanadate-binding site in TRPM4 (Winkler et al., 2017). Moreover, together with mutagenesis, structures of TRPML channels also reveal how phosphoinositides, which bind to a pocket just beneath the inner membrane, allosterically regulate the pore of these channels (Fine et al., 2018). Of note, TRPML and TRPP channels feature a large luminal or extracellular domain, collectively called polycystin-mucolipin domain (PMD), which is absent in other TRP subfamilies and related VGICs. The PMD domain sits atop and

strategically interacts with the transmembrane core, giving an immediate impression that this domain may recognize as yet unidentified ligand(s) and/or respond to physical force to allosterically gate these channels (Shen et al., 2016; Chen et al., 2017; Grieben et al., 2017; Hirschi et al., 2017; Schmiede et al., 2017; Wilkes et al., 2017; Zhou et al., 2017). Indeed, protonation of the luminal loop on PMD regulates TRPML channels (Li et al., 2017). In both TRPC3 and TRPC6, the S3 helix extends into the extracellular space and, together with the neighboring S1-S2 and S3-S4 loops, forms a distinct extracellular domain (Azumaya et al., 2018; Fan et al., 2018; Sierra-Valdez et al., 2018; Tang et al., 2018). This structure interacts with the channel pore, implying that it may regulate channel function upon receiving external stimuli and confer drug sensitivity. Finally, in the mechanosensitive no mechanoreceptor potential C channel, 29 ankyrin repeats form a helical spring structure in cytosol, supporting the hypothesis that these ankyrin repeats, when anchored to cytoskeleton, can function as an elastic tether that would transduce mechanical displacement to the ion channel gate (Jin et al., 2017).

Temperature sensing in TRP channels

In addition to sensing chemical ligands and mechanical force, a subset of mammalian TRP channels can be directly activated by cold (TRPA1, although debatable), cool (TRPM8 and TRPC5), warm (TRPV3, TRPV4, TRPM2, TRPM4, and TRPM5), hot (TRPV1 and TRPM3), or extreme hot (TRPV2) temperatures (Caterina et al., 1997, 1999; McKemy et al., 2002; Peier et al., 2002a, b; Smith et al., 2002; Xu et al., 2002; Chung et al., 2003; Story et al., 2003; Jordt et al., 2004; Talavera et al., 2005; Vriens et al., 2011; Zimmermann et al., 2011; Song et al., 2016; Tan and McNaughton, 2016). Some of these thermo-sensitive TRP channels, such as TRPV1, TRPM8, TRPA1, TRPM2, and TRPM3, function as molecular thermometers for detecting environment and body temperatures, which is essential for us to avoid damaging temperature extremes and to maintain body temperature within a narrow physiological range (Caterina et al., 2000; Davis et al., 2000; Bautista et al., 2007; Colburn et al., 2007; Dhaka et al., 2007; Vriens et al., 2011; Song et al., 2016; Tan and McNaughton, 2016; Vandewauw et al., 2018). Interestingly, TRPV1 in ground squirrels and camels exhibits diminished heat sensitivity, allowing them to tolerate high temperatures and inhabit otherwise inhospitable ecological niches (Laursen et al., 2016). In the same vein, a TRPV1 splice variant in vampire bats activates in much lower temperatures, which may underlie its role in sensing infrared radiation (Gracheva et al., 2011). TRP channels also play pivotal roles in thermosensation in lower organisms. For instance, TRPA1 is expressed in the pit organ of some snakes, where it is activated by heat in the form of infrared radiation for detection of warm-blooded predators or prey (Gracheva et al., 2010). Similarly, in insects such as flies and mosquitos, TRPA1 also serves as a warm sensor and controls their temperature preference behavior (Viswanath et al., 2003; Hamada et al., 2008; Wang et al., 2009). Taken together, these studies demonstrate fundamental roles of TRP channels in thermosensation in both mammals and lower organisms and highlight how adaptive diversification and tuning of TRP

channel thermal sensitivity can accommodate special needs and variations in environment niches of different organisms.

However, how an ion channel acquires steep temperature sensitivity is a much tougher nut to crack than understanding ligand- or voltage-gated ion channels. Chemical ligands or voltage can be at least conceptually understood to either snugly fit into a pocket in a lock-and-key mechanism or exert electric force on membrane-embedded gating charges, respectively. In contrast, thermal stimuli, being ubiquitous, are not confined to a discrete domain(s), and thus can exert global effects on protein structures. Indeed, TRPV3 structures determined at different temperatures show conformational changes in both transmembrane and cytosolic domains upon heat activation (Singh et al., 2019). Moreover, in the most extensively studied heat-activated TRPV1 channel, various domains dispersed throughout the entire primary sequence have been identified to contribute to thermal activation (Brauchi et al., 2006; Yao et al., 2011; Laursen et al., 2016; Liu and Qin, 2017; Sosa-Pagán et al., 2017; Zhang et al., 2018a); these domains either directly sense thermal stimuli or couple the conformational changes in heat sensor to subsequent gate opening. Intriguingly, repetitive heat activation of TRPV1 leads to irreversible channel inactivation via a mechanism possibly analogous to partial denaturation of several regions of the channel (Sánchez-Moreno et al., 2018), in support of a global effect of heat on channel structure.

None of the available TRPV1 structures has been determined at different temperatures so far, so they are silent on heat-associated conformational changes. Nonetheless, molecular dynamic simulation of the TRPV1 channel has yielded several principles that are consistent with a large body of mutagenesis and structural studies (Fig. 7 A; Zheng and Qin, 2015; Chugunov et al., 2016; Wen et al., 2016; Melnick and Kaviany, 2018; Wen and Zheng, 2018; Ladrón-de-Guevara et al., 2019). First, besides serving as a substrate site for chemical ligands (e.g., ions, protons, and spider toxins), the TRPV1 outer pore region was shown to contribute to heat activation. For instance, the TRPV1 turret region, which immediately precedes the pore helix, was shown to regulate channel thermal sensitivity (Yang et al., 2010; Yao et al., 2010; Jara-Oseguera et al., 2016). In addition, mutations in the outer pore region of TRPV3 similarly abolish heat activation without perturbing sensitivity to various chemical agonists (Grandl et al., 2008). Moreover, several residues in an outer pore loop of both TRPV1 and TRPV3 change their accessibility to solvent upon heat activation, further supporting a role for the outer pore region in thermal activation of these channels (Kim et al., 2013). More recently, it has been shown that grafting the pore domain of TRPV1 into the Shaker K_v channel confers heat sensitivity to the otherwise temperature-insensitive channel (Zhang et al., 2018a). Consistent with these mutagenesis studies, molecular dynamic stimulation predicts heat-induced destabilization of hydrophobic clusters within the outer pore region, lending support to the heat capacity theory that hypothesizes that exposure of 20–25 hydrophobic residues per subunit to solvent gives rise to heat sensitivity (Clapham and Miller, 2011). Second, molecular dynamic studies also support the hypothesis that a resident phosphoinositide lipid is ejected from the vanilloid pocket upon heating, resulting in conformational rearrangements

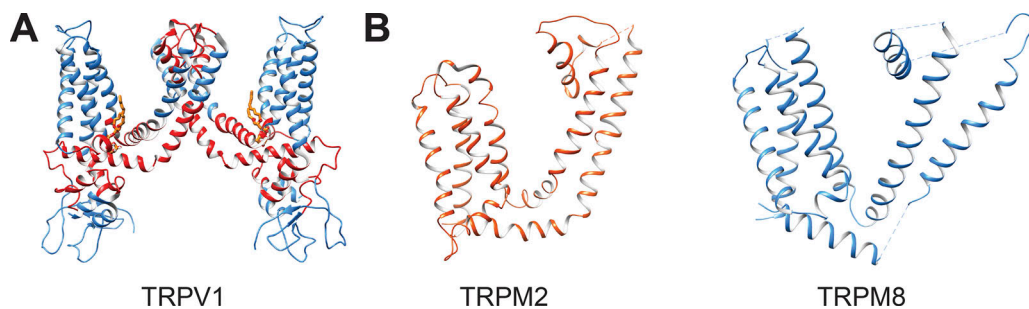


Figure 7. Structures of thermo-sensitive TRP channels. (A) Two diagonally apposed TRPV1 subunits are shown in ribbon diagram, with regions proposed to undergo heat-evoked conformational changes highlighted with red. The phosphoinositide lipid predicted to be ejected from the vanilloid pocket upon heating is shown in sticks. **(B)** Comparison of structures of warm-activated TRPM2 and cold-activated TRPM8. Only the transmembrane region of one subunit is shown here. Unlike other TRP channels, TRPM8 lacks the helical S4–S5 linker and a structurally defined selectivity filter in a closed state, hinting at structural flexibility of these structural elements. PDB accession nos. are as follows: TRPV1 (5IRX), TRPM2 (6MIX), and TRPM8 (6BPQ).

around the pocket that then propagate to and ultimately open the pore (Gao et al., 2016). Finally, heat further evokes conformational changes within several cytoplasmic structures, including the membrane proximal domain, C-terminal domain, and the S2–S3 loop. Of note, protein kinase C (PKC)-mediated phosphorylation of Ser502, which resides precisely at the S2–S3 loop, has been reported to enhance thermal sensitivity of TRPV1 (Premkumar and Ahern, 2000; Numazaki et al., 2002). Indeed, this may represent a major mechanism whereby inflammatory mediators (e.g., bradykinin) produce thermal hyperalgesia via PKC activation.

How the TRPM8 channel is activated by cold stimuli is even more mysterious. Intriguingly, within the TRPM subfamily, to which TRPM8 belongs, TRPM2 and TRPM3 are activated by warm and hot temperatures (Vriens et al., 2011; Song et al., 2016; Tan and McNaughton, 2016), respectively. Comparison of TRPM8 and TRPM2 structures shows that they differ in organization of two domains within an otherwise similar overall architecture, including both harboring a similar Ca^{2+} -regulatory site (Fig. 7 B; Huang et al., 2018; Wang et al., 2018; Yin et al., 2018). First, TRPM8 conspicuously lacks the helical S4–S5 linker in closed state that is critical for gating of most TRP channels and instead harbors a short loop connecting the S4 and S5 helices. Second, the selectivity filter and outer pore loops of TRPM8 are surprisingly invisible in a closed state. Interestingly, both the S4–S5 linker and selectivity filter are well-defined in a desensitized state in TRPM8 (Diver et al., 2019), hinting that these structure elements are likely more dynamic as compared to TRPM2 channels. Whether such structural differences reflect a genuinely distinct design principle for cold- and heat-sensitive TRPM channels remains to be determined.

Concluding remarks

When the TRPV1 structures were first reported in 2013, it was impossible to imagine that, seven years later, structures have been determined for at least one member of every subfamily of TRP channels. With continuous improvement in single-particle cryo-EM and development of novel amphiphiles, detergents, and nanodisc technology for stabilizing membrane proteins, more TRP channel structures are certainly forthcoming. Single-particle cryo-EM, in essence, is a single-molecule method and

in theory can deliver multiple structures representing distinct conformational states of a given protein from the same dataset. However, in practice, conformational heterogeneity often leads to lower-resolution structures as failure to accurately classify particles into separate groups will blur conformational dynamic regions. Indeed, developing novel algorithms for classifying heterogeneous samples and defining their conformational landscapes is an actively pursued research frontier of single-particle cryo-EM (Frank and Ourmazd, 2016; Nakane et al., 2018).

We now know the structural blueprint of each subtype of TRP channels, but how most TRP channels are activated or regulated remains enigmatic. This is an extremely challenging question to address because, in contrast to VGICs, where rich pharmacological tools have greatly advanced our understanding of fundamental principles that underlie ion permeation and regulation of these channels, pharmacology for most TRP channels is still in its infancy. Consequently, we lack tool compounds and peptide toxins to trap TRP channels in distinct functional states for structure determination so as to fully appreciate the range of conformations that certainly exist to account for the complex regulatory and activation mechanisms exhibited by these poly-modal cellular sensors. I hope that pharmacological discoveries from academic laboratories and drug development campaigns of pharmaceutical companies will identify novel small molecule compounds, peptide toxins, or conformation-sensitive antibodies that can modulate TRP channel function. Such pharmacological tools will prove indispensable for further advancing TRP channel structural biology. Finally, as is true for many other ion channels, it is often difficult to unambiguously correlate a TRP channel structure with a certain functional state along its gating cycle. Therefore, other methods, such as molecular dynamics simulation and single-molecule FRET (Zheng and Qin, 2015; Zagotta et al., 2016; Gordon et al., 2018; Yang et al., 2018), should be used to study structural dynamics of TRP channels.

Acknowledgments

Lesley C. Anson served as guest editor.

The author is enormously grateful to Lesley Anson for her invaluable editorial support throughout the process.

This work has been supported by the National Institutes of Health RO1 DK110575 grant and the U.S. Department of Defense W81XWH-17-1-0158 discovery award to E. Cao, and E. Cao is a Pew Scholar supported by the Pew Charitable Trusts.

The author declares no competing financial interests.

Submitted: 29 April 2019

Accepted: 3 January 2020

References

- Adrian, M., J. Dubochet, J. Lepault, and A.W. McDowell. 1984. Cryo-electron microscopy of viruses. *Nature*. 308:32–36. <https://doi.org/10.1038/308032a0>
- Aggarwal, S.K., and R. MacKinnon. 1996. Contribution of the S4 segment to gating charge in the Shaker K⁺ channel. *Neuron*. 16:1169–1177. [https://doi.org/10.1016/S0896-6273\(00\)80143-9](https://doi.org/10.1016/S0896-6273(00)80143-9)
- Agrawal, R.K., and J. Frank. 1999. Structural studies of the translational apparatus. *Curr. Opin. Struct. Biol.* 9:215–221. [https://doi.org/10.1016/S0959-440X\(99\)80031-1](https://doi.org/10.1016/S0959-440X(99)80031-1)
- Alabi, A.A., M.I. Bahamonde, H.J. Jung, J.I. Kim, and K.J. Swartz. 2007. Portability of paddle motif function and pharmacology in voltage sensors. *Nature*. 450:370–375. <https://doi.org/10.1038/nature06266>
- Almers, W., and E.W. McCleskey. 1984. Non-selective conductance in calcium channels of frog muscle: calcium selectivity in a single-file pore. *J. Physiol.* 353:585–608. <https://doi.org/10.1113/jphysiol.1984.sp015352>
- Andreev, Y.A., S.A. Kozlov, S.G. Koshelev, E.A. Ivanova, M.M. Monastyrnaya, E.P. Kozlovskaya, and E.V. Grishin. 2008. Analgesic compound from sea anemone *Heteractis crispa* is the first polypeptide inhibitor of vanilloid receptor 1 (TRPV1). *J. Biol. Chem.* 283:23914–23921. <https://doi.org/10.1074/jbc.M800776200>
- Arif Pavel, M., C. Lv, C. Ng, L. Yang, P. Kashyap, C. Lam, V. Valentino, H.Y. Fung, T. Campbell, S.G. Møller, et al. 2016. Function and regulation of TRPP2 ion channel revealed by a gain-of-function mutant. *Proc. Natl. Acad. Sci. USA*. 113:E2363–E2372. <https://doi.org/10.1073/pnas.1517066113>
- Armstrong, C.M. 1971. Interaction of tetraethylammonium ion derivatives with the potassium channels of giant axons. *J. Gen. Physiol.* 58:413–437. <https://doi.org/10.1085/jgp.58.4.413>
- Autzen, H.E., A.G. Myasnikov, M.G. Campbell, D. Asarnow, D. Julius, and Y. Cheng. 2018. Structure of the human TRPM4 ion channel in a lipid nanodisc. *Science*. 359:228–232. <https://doi.org/10.1126/science.aar4510>
- Azumaya, C.M., F. Sierra-Valdez, J.F. Cordero-Morales, and T. Nakagawa. 2018. Cryo-EM structure of the cytoplasmic domain of murine transient receptor potential cation channel subfamily C member 6 (TRPC6). *J. Biol. Chem.* 293:10381–10391. <https://doi.org/10.1074/jbc.RA118.003183>
- Bae, C., C. Anselmi, J. Kalia, A. Jara-Oseguera, C.D. Schwieters, D. Krepiak, C. Won Lee, E.H. Kim, J.I. Kim, J.D. Faraldo-Gómez, and K.J. Swartz. 2016. Structural insights into the mechanism of activation of the TRPV1 channel by a membrane-bound tarantula toxin. *eLife*. 5:e11273. <https://doi.org/10.7554/eLife.11273>
- Banerjee, A., A. Lee, E. Campbell, and R. MacKinnon. 2013. Structure of a pore-blocking toxin in complex with a eukaryotic voltage-dependent K⁽⁺⁾ channel. *eLife*. 2:e00594. <https://doi.org/10.7554/eLife.00594>
- Bautista, D.M., J. Siemens, J.M. Glazer, P.R. Tsuruda, A.I. Basbaum, C.L. Stucky, S.E. Jordt, and D. Julius. 2007. The menthol receptor TRPM8 is the principal detector of environmental cold. *Nature*. 448:204–208. <https://doi.org/10.1038/nature05910>
- Bezanilla, F. 2018. Gating currents. *J. Gen. Physiol.* 150:911–932. <https://doi.org/10.1085/jgp.201812090>
- Bohlen, C.J., A. Priel, S. Zhou, D. King, J. Siemens, and D. Julius. 2010. A bivalent tarantula toxin activates the capsaicin receptor, TRPV1, by targeting the outer pore domain. *Cell*. 141:834–845. <https://doi.org/10.1016/j.cell.2010.03.052>
- Bosmans, F., M.F. Martin-Eauclaire, and K.J. Swartz. 2008. Deconstructing voltage sensor function and pharmacology in sodium channels. *Nature*. 456:202–208. <https://doi.org/10.1038/nature07473>
- Brauchi, S., P. Orío, and R. Latorre. 2004. Clues to understanding cold sensation: thermodynamics and electrophysiological analysis of the cold receptor TRPM8. *Proc. Natl. Acad. Sci. USA*. 101:15494–15499. <https://doi.org/10.1073/pnas.0406773101>
- Brauchi, S., G. Orta, M. Salazar, E. Rosenmann, and R. Latorre. 2006. A hot-sensing cold receptor: C-terminal domain determines thermosensation in transient receptor potential channels. *J. Neurosci.* 26:4835–4840. <https://doi.org/10.1523/JNEUROSCI.5080-05.2006>
- Callaway, E. 2015. The revolution will not be crystallized: a new method sweeps through structural biology. *Nature*. 525:172–174. <https://doi.org/10.1038/525172a>
- Campbell, M.G., A. Cheng, A.F. Brilot, A. Moeller, D. Lyumkis, D. Veesler, J. Pan, S.C. Harrison, C.S. Potter, B. Carragher, and N. Grigorieff. 2012. Movies of ice-embedded particles enhance resolution in electron cryo-microscopy. *Structure*. 20:1823–1828. <https://doi.org/10.1016/j.str.2012.08.026>
- Canul-Sánchez, J.A., I. Hernández-Araiza, E. Hernández-García, I. Llorente, S.L. Morales-Lázaro, L.D. Islas, and T. Rosenbaum. 2018. Different agonists induce distinct single-channel conductance states in TRPV1 channels. *J. Gen. Physiol.* 150:1735–1746. <https://doi.org/10.1085/jgp.201812141>
- Cao, E., M. Liao, Y. Cheng, and D. Julius. 2013. TRPV1 structures in distinct conformations reveal activation mechanisms. *Nature*. 504:113–118. <https://doi.org/10.1038/nature12823>
- Caterina, M.J., M.A. Schumacher, M. Tominaga, T.A. Rosen, J.D. Levine, and D. Julius. 1997. The capsaicin receptor: a heat-activated ion channel in the pain pathway. *Nature*. 389:816–824. <https://doi.org/10.1038/39807>
- Caterina, M.J., T.A. Rosen, M. Tominaga, A.J. Brake, and D. Julius. 1999. A capsaicin-receptor homologue with a high threshold for noxious heat. *Nature*. 398:436–441. <https://doi.org/10.1038/18906>
- Caterina, M.J., A. Leffler, A.B. Malmberg, W.J. Martin, J. Traffon, K.R. Petersen-Zeit, M. Koltzenburg, A.I. Basbaum, and D. Julius. 2000. Impaired nociception and pain sensation in mice lacking the capsaicin receptor. *Science*. 288:306–313. <https://doi.org/10.1126/science.288.5464.306>
- Catterall, W.A. 1986. Molecular properties of voltage-sensitive sodium channels. *Annu. Rev. Biochem.* 55:953–985. <https://doi.org/10.1146/annurev.bi.55.070186.004513>
- Catterall, W.A. 2010. Ion channel voltage sensors: structure, function, and pathophysiology. *Neuron*. 67:915–928. <https://doi.org/10.1016/j.neuron.2010.08.021>
- Catterall, W.A., S. Cestèle, V. Yarov-Yarovoy, F.H. Yu, K. Konoki, and T. Scheuer. 2007. Voltage-gated ion channels and gating modifier toxins. *Toxicol.* 49:124–141. <https://doi.org/10.1016/j.toxicol.2006.09.022>
- Chen, Q., J. She, W. Zeng, J. Guo, H. Xu, X.C. Bai, and Y. Jiang. 2017. Structure of mammalian endolysosomal TRPML1 channel in nanodiscs. *Nature*. 550:415–418. <https://doi.org/10.1038/nature24035>
- Chou, M.Z., T. Mtui, Y.D. Gao, M. Kohler, and R.E. Middleton. 2004. Resiniferatoxin binds to the capsaicin receptor (TRPV1) near the extracellular side of the S4 transmembrane domain. *Biochemistry*. 43:2501–2511. <https://doi.org/10.1021/bi035981h>
- Christensen, A.P., N. Akyuz, and D.P. Corey. 2016. The Outer Pore and Selectivity Filter of TRPA1. *PLoS One*. 11:e0166167. <https://doi.org/10.1371/journal.pone.0166167>
- Chugunov, A.O., P.E. Volynsky, N.A. Krylov, D.E. Nolde, and R.G. Efremov. 2016. Temperature-sensitive gating of TRPV1 channel as probed by atomistic simulations of its trans- and juxtamembrane domains. *Sci. Rep.* 6:33112. <https://doi.org/10.1038/srep33112>
- Chung, M.K., H. Lee, and M.J. Caterina. 2003. Warm temperatures activate TRPV4 in mouse 308 keratinocytes. *J. Biol. Chem.* 278:32037–32046. <https://doi.org/10.1074/jbc.M303251200>
- Chung, M.K., A.D. Güler, and M.J. Caterina. 2008. TRPV1 shows dynamic ionic selectivity during agonist stimulation. *Nat. Neurosci.* 11:555–564. <https://doi.org/10.1038/nn.2102>
- Clapham, D.E., and C. Miller. 2011. A thermodynamic framework for understanding temperature sensing by transient receptor potential (TRP) channels. *Proc. Natl. Acad. Sci. USA*. 108:19492–19497. <https://doi.org/10.1073/pnas.1117485108>
- Colburn, R.W., M.L. Lubin, D.J. Stone Jr., Y. Wang, D. Lawrence, M.R. D'Andrea, M.R. Brandt, Y. Liu, C.M. Flores, and N. Qin. 2007. Attenuated cold sensitivity in TRPM8 null mice. *Neuron*. 54:379–386. <https://doi.org/10.1016/j.neuron.2007.04.017>
- Cooley, R.B., D.J. Arp, and P.A. Karplus. 2010. Evolutionary origin of a secondary structure: π -helices as cryptic but widespread insertional variations of α -helices that enhance protein functionality. *J. Mol. Biol.* 404:232–246. <https://doi.org/10.1016/j.jmb.2010.09.034>

- Cuyppers, E., A. Yanagihara, E. Karlsson, and J. Tytgat. 2006. Jellyfish and other cnidarian envenomations cause pain by affecting TRPV1 channels. *FEBS Lett.* 580:5728–5732. <https://doi.org/10.1016/j.febslet.2006.09.030>
- Dang, S., M.K. van Goor, D. Asarnow, Y. Wang, D. Julius, Y. Cheng, and J. van der Wijk. 2019. Structural insight into TRPV5 channel function and modulation. *Proc. Natl. Acad. Sci. USA.* 116:8869–8878. <https://doi.org/10.1073/pnas.1820323116>
- Davis, J.B., J. Gray, M.J. Gunthorpe, J.P. Hatcher, P.T. Davey, P. Overend, M.H. Harries, J. Latcham, C. Clapham, K. Atkinson, et al. 2000. Vanilloid receptor-1 is essential for inflammatory thermal hyperalgesia. *Nature.* 405:183–187. <https://doi.org/10.1038/35012076>
- DeCaen, P.G., X. Liu, S. Abiria, and D.E. Clapham. 2016. Atypical calcium regulation of the PKD2-L1 polycystin ion channel. *eLife.* 5:e13413. <https://doi.org/10.7554/eLife.13413>
- Deng, Z., N. Paknejad, G. Maksaev, M. Sala-Rabanal, C.G. Nichols, R.K. Hite, and P. Yuan. 2018. Cryo-EM and X-ray structures of TRPV4 reveal insight into ion permeation and gating mechanisms. *Nat. Struct. Mol. Biol.* 25:252–260. <https://doi.org/10.1038/s41594-018-0037-5>
- Dhaka, A., A.N. Murray, J. Mathur, T.J. Earley, M.J. Petrus, and A. Patapoutian. 2007. TRPM8 is required for cold sensation in mice. *Neuron.* 54:371–378. <https://doi.org/10.1016/j.neuron.2007.02.024>
- Diver, M.M., Y. Cheng, and D. Julius. 2019. Structural insights into TRPM8 inhibition and desensitization. *Science.* 365:1434–1440. <https://doi.org/10.1126/science.aax6672>
- Dosey, T.L., Z. Wang, G. Fan, Z. Zhang, I.I. Serysheva, W. Chiu, and T.G. Wensel. 2019. Structures of TRPV2 in distinct conformations provide insight into role of the pore turret. *Nat. Struct. Mol. Biol.* 26:40–49. <https://doi.org/10.1038/s41594-018-0168-8>
- Doyle, D.A., J. Morais Cabral, R.A. Pfuetzner, A. Kuo, J.M. Gulbis, S.L. Cohen, B.T. Chait, and R. MacKinnon. 1998. The structure of the potassium channel: molecular basis of K⁺ conduction and selectivity. *Science.* 280:69–77. <https://doi.org/10.1126/science.280.5360.69>
- Duan, J., J. Li, B. Zeng, G.L. Chen, X. Peng, Y. Zhang, J. Wang, D.E. Clapham, Z. Li, and J. Zhang. 2018a. Structure of the mouse TRPC4 ion channel. *Nat. Commun.* 9:3102. <https://doi.org/10.1038/s41467-018-05247-9>
- Duan, J., Z. Li, J. Li, R.E. Hulse, A. Santa-Cruz, W.C. Valinsky, S.A. Abiria, G. Kravinsky, J. Zhang, and D.E. Clapham. 2018b. Structure of the mammalian TRPM7, a magnesium channel required during embryonic development. *Proc. Natl. Acad. Sci. USA.* 115:E8201–E8210. <https://doi.org/10.1073/pnas.1810719115>
- Duan, J., Z. Li, J. Li, A. Santa-Cruz, S. Sanchez-Martinez, J. Zhang, and D.E. Clapham. 2018c. Structure of full-length human TRPM4. *Proc. Natl. Acad. Sci. USA.* 115:2377–2382. <https://doi.org/10.1073/pnas.1722038115>
- Enkhbayar, P., K. Hikichi, M. Osaki, R.H. Kretsinger, and N. Matsushima. 2006. 3(10)-helices in proteins are parhelices. *Proteins.* 64:691–699. <https://doi.org/10.1002/prot.21026>
- Fan, C., W. Choi, W. Sun, J. Du, and W. Lü. 2018. Structure of the human lipid-gated cation channel TRPC3. *eLife.* 7:e36852. <https://doi.org/10.7554/eLife.36852>
- Fernández-Mariño, A.I., T.J. Harpole, K. Oelstrom, L. Delemotte, and B. Chanda. 2018. Gating interaction maps reveal a noncanonical electro-mechanical coupling mode in the Shaker K⁺ channel. *Nat. Struct. Mol. Biol.* 25:320–326. <https://doi.org/10.1038/s41594-018-0047-3>
- Fine, M., P. Schmiede, and X. Li. 2018. Structural basis for PtdInsP₂-mediated human TRPML1 regulation. *Nat. Commun.* 9:4192. <https://doi.org/10.1038/s41467-018-06493-7>
- Frank, J., and A. Ourmazd. 2016. Continuous changes in structure mapped by manifold embedding of single-particle data in cryo-EM. *Methods.* 100:61–67. <https://doi.org/10.1016/j.jymeth.2016.02.007>
- Frank, J., M. Radermacher, P. Penczek, J. Zhu, Y. Li, M. Ladjadj, and A. Leith. 1996. SPIDER and WEB: processing and visualization of images in 3D electron microscopy and related fields. *J. Struct. Biol.* 116:190–199. <https://doi.org/10.1006/jsbi.1996.0030>
- Fujimoto, C., Y. Ishimaru, Y. Katano, T. Misaka, T. Yamasoba, T. Asakura, and K. Abe. 2011. The single pore residue Asp523 in PKD2L1 determines Ca²⁺ permeation of the PKDIL3/PKD2L1 complex. *Biochem. Biophys. Res. Commun.* 404:946–951. <https://doi.org/10.1016/j.bbrc.2010.12.086>
- Gao, Y., E. Cao, D. Julius, and Y. Cheng. 2016. TRPV1 structures in nanodiscs reveal mechanisms of ligand and lipid action. *Nature.* 534:347–351. <https://doi.org/10.1038/nature17964>
- Gavva, N.R., L. Klionsky, Y. Qu, L. Shi, R. Tamir, S. Edenson, T.J. Zhang, V.N. Viswanadhan, A. Toth, L.V. Pearce, et al. 2004. Molecular determinants of vanilloid sensitivity in TRPV1. *J. Biol. Chem.* 279:20283–20295. <https://doi.org/10.1074/jbc.M312577200>
- Geron, M., R. Kumar, W. Zhou, J.D. Faraldo-Gómez, V. Vásquez, and A. Priel. 2018. TRPV1 pore turret dictates distinct DkTx and capsaicin gating. *Proc. Natl. Acad. Sci. USA.* 115:E11837–E11846. <https://doi.org/10.1073/pnas.1809662115>
- Gordon, S.E., M. Munari, and W.N. Zagotta. 2018. Visualizing conformational dynamics of proteins in solution and at the cell membrane. *eLife.* 7:e37248.
- Gracheva, E.O., N.T. Ingolia, Y.M. Kelly, J.F. Cordero-Morales, G. Holloper, A.T. Chesler, E.E. Sánchez, J.C. Perez, J.S. Weissman, and D. Julius. 2010. Molecular basis of infrared detection by snakes. *Nature.* 464:1006–1011. <https://doi.org/10.1038/nature08943>
- Gracheva, E.O., J.F. Cordero-Morales, J.A. González-Carcacia, N.T. Ingolia, C. Manno, C.I. Aranguren, J.S. Weissman, and D. Julius. 2011. Ganglion-specific splicing of TRPV1 underlies infrared sensation in vampire bats. *Nature.* 476:88–91. <https://doi.org/10.1038/nature10245>
- Grandl, J., H. Hu, M. Bandell, B. Bursulaya, M. Schmidt, M. Petrus, and A. Patapoutian. 2008. Pore region of TRPV3 ion channel is specifically required for heat activation. *Nat. Neurosci.* 11:1007–1013. <https://doi.org/10.1038/nn.2169>
- Grieben, M., A.C. Pike, C.A. Shintre, E. Venturi, S. El-Ajoui, A. Tessitore, L. Shrestha, S. Mukhopadhyay, P. Mahajan, R. Chalk, et al. 2017. Structure of the polycystic kidney disease TRP channel Polycystin-2 (PC2). *Nat. Struct. Mol. Biol.* 24:114–122. <https://doi.org/10.1038/nsmb.3343>
- Grigorieff, N. 2007. FREALIGN: high-resolution refinement of single particle structures. *J. Struct. Biol.* 157:117–125. <https://doi.org/10.1016/j.jsb.2006.05.004>
- Grigorieff, N., and S.C. Harrison. 2011. Near-atomic resolution reconstructions of icosahedral viruses from electron cryo-microscopy. *Curr. Opin. Struct. Biol.* 21:265–273. <https://doi.org/10.1016/j.sbi.2011.01.008>
- Guo, J., J. She, W. Zeng, Q. Chen, X.C. Bai, and Y. Jiang. 2017. Structures of the calcium-activated, non-selective cation channel TRPM4. *Nature.* 552:205–209. <https://doi.org/10.1038/nature24997>
- Hamada, F.N., M. Rosenzweig, K. Kang, S.R. Pulver, A. Ghezzi, T.J. Jegla, and P.A. Garrity. 2008. An internal thermal sensor controlling temperature preference in *Drosophila*. *Nature.* 454:217–220. <https://doi.org/10.1038/nature07001>
- Hardie, R.C., and B. Minke. 1993. Novel Ca²⁺ channels underlying transduction in *Drosophila* photoreceptors: implications for phosphoinositide-mediated Ca²⁺ mobilization. *Trends Neurosci.* 16:371–376. [https://doi.org/10.1016/0166-2236\(93\)90095-4](https://doi.org/10.1016/0166-2236(93)90095-4)
- Henderson, R. 1995. The potential and limitations of neutrons, electrons and X-rays for atomic resolution microscopy of unstained biological molecules. *Q. Rev. Biophys.* 28:171–193. <https://doi.org/10.1017/S00335835000305X>
- Hess, P., and R.W. Tsien. 1984. Mechanism of ion permeation through calcium channels. *Nature.* 309:453–456. <https://doi.org/10.1038/309453a0>
- Hibbs, R.E., and E. Gouaux. 2011. Principles of activation and permeation in an anion-selective Cys-loop receptor. *Nature.* 474:54–60. <https://doi.org/10.1038/nature10139>
- Hille, B. 1971. The permeability of the sodium channel to organic cations in myelinated nerve. *J. Gen. Physiol.* 58:599–619. <https://doi.org/10.1085/jgp.58.6.599>
- Hille, B. 1972. The permeability of the sodium channel to metal cations in myelinated nerve. *J. Gen. Physiol.* 59:637–658. <https://doi.org/10.1085/jgp.59.6.637>
- Hirschi, M., M.A. Herzik Jr., J. Wie, Y. Suo, W.F. Borschel, D. Ren, G.C. Lander, and S.Y. Lee. 2017. Cryo-electron microscopy structure of the lysosomal calcium-permeable channel TRPML3. *Nature.* 550:411–414. <https://doi.org/10.1038/nature24055>
- Hofmann, T., V. Chubanov, T. Gudermann, and C. Montell. 2003. TRPM5 is a voltage-modulated and Ca(2+)-activated monovalent selective cation channel. *Curr. Biol.* 13:1153–1158. [https://doi.org/10.1016/S0960-9822\(03\)00431-7](https://doi.org/10.1016/S0960-9822(03)00431-7)
- Hong, C., M. Kwak, J. Myeong, K. Ha, J. Wie, J.H. Jeon, and I. So. 2015. Extracellular disulfide bridges stabilize TRPC5 dimerization, trafficking, and activity. *Pflugers Arch.* 467:703–712. <https://doi.org/10.1007/s00424-014-1540-0>
- Hoshi, T., W.N. Zagotta, and R.W. Aldrich. 1990. Biophysical and molecular mechanisms of Shaker potassium channel inactivation. *Science.* 250:533–538. <https://doi.org/10.1126/science.2122519>
- Huang, Y., P.A. Winkler, W. Sun, W. Lü, and J. Du. 2018. Architecture of the TRPM2 channel and its activation mechanism by ADP-ribose and calcium. *Nature.* 562:145–149. <https://doi.org/10.1038/s41586-018-0558-4>
- Hughes, T.E.T., D.T. Lodowski, K.W. Huynh, A. Yazici, J. Del Rosario, A. Kapoor, S. Basak, A. Samanta, X. Han, S. Chakrapani, et al. 2018a.

- Structural basis of TRPV5 channel inhibition by econazole revealed by cryo-EM. *Nat. Struct. Mol. Biol.* 25:53–60. <https://doi.org/10.1038/s41594-017-0009-1>
- Hughes, T.E.T., R.A. Pumroy, A.T. Yazici, M.A. Kasimova, E.C. Fluck, K.W. Huynh, A. Samanta, S.K. Molugu, Z.H. Zhou, V. Carnevale, et al. 2018b. Structural insights on TRPV5 gating by endogenous modulators. *Nat. Commun.* 9:4198. <https://doi.org/10.1038/s41467-018-06753-6>
- Hughes, T.E., J.S. Del Rosario, A. Kapoor, A.T. Yazici, Y. Yudin, E.C. Fluck III, M. Filizola, T. Rohacs, and V.Y. Moiseenkova-Bell. 2019. Structure-based characterization of novel TRPV5 inhibitors. *eLife*. 8:e49572. <https://doi.org/10.7554/eLife.49572>
- Hui, K., B. Liu, and F. Qin. 2003. Capsaicin activation of the pain receptor, VR1: multiple open states from both partial and full binding. *Biophys. J.* 84:2957–2968. [https://doi.org/10.1016/S0006-3495\(03\)70022-8](https://doi.org/10.1016/S0006-3495(03)70022-8)
- Hulse, R.E., Z. Li, R.K. Huang, J. Zhang, and D.E. Clapham. 2018. Cryo-EM structure of the polycystin 2-11 ion channel. *eLife*. 7:e36931. <https://doi.org/10.7554/eLife.36931>
- Jara-Oseguera, A., C. Bae, and K.J. Swartz. 2016. An external sodium ion binding site controls allosteric gating in TRPV1 channels. *eLife*. 5:e13356. <https://doi.org/10.7554/eLife.13356>
- Jara-Oseguera, A., K.E. Huffer, and K.J. Swartz. 2019. The ion selectivity filter is not an activation gate in TRPV1-3 channels. *eLife*. 8:e51212. <https://doi.org/10.7554/eLife.51212>
- Jiang, Y., A. Lee, J. Chen, M. Cadene, B.T. Chait, and R. MacKinnon. 2002. The open pore conformation of potassium channels. *Nature*. 417:523–526. <https://doi.org/10.1038/417523a>
- Jiang, D., H. Shi, L. Tonggu, T.M. Gamal El-Din, M.J. Lenaeus, Y. Zhao, C. Yoshioka, N. Zheng, and W.A. Catterall. 2019. Structure of the Cardiac Sodium Channel. *Cell*. 180:122–134. <https://doi.org/10.1016/j.cell.2019.11.041>
- Jin, P., D. Bulkley, Y. Guo, W. Zhang, Z. Guo, W. Huynh, S. Wu, S. Meltzer, T. Cheng, L.Y. Jan, et al. 2017. Electron cryo-microscopy structure of the mechanotransduction channel NOMPC. *Nature*. 547:118–122. <https://doi.org/10.1038/nature22981>
- Jordt, S.E., and D. Julius. 2002. Molecular basis for species-specific sensitivity to “hot” chili peppers. *Cell*. 108:421–430. [https://doi.org/10.1016/S0092-8674\(02\)00637-2](https://doi.org/10.1016/S0092-8674(02)00637-2)
- Jordt, S.E., M. Tominaga, and D. Julius. 2000. Acid potentiation of the capsaicin receptor determined by a key extracellular site. *Proc. Natl. Acad. Sci. USA*. 97:8134–8139. <https://doi.org/10.1073/pnas.100129497>
- Jordt, S.E., D.M. Bautista, H.H. Chuang, D.D. McKemy, P.M. Zygmunt, E.D. Högestätt, I.D. Meng, and D. Julius. 2004. Mustard oils and cannabinoids excite sensory nerve fibres through the TRP channel ANKTM1. *Nature*. 427:260–265. <https://doi.org/10.1038/nature02282>
- Jorgensen, C., S. Furini, and C. Domene. 2016. Energetics of Ion Permeation in an Open-Activated TRPV1 Channel. *Biophys. J.* 111:1214–1222. <https://doi.org/10.1016/j.bpj.2016.08.009>
- Kalia, J., M. Milescu, J. Salvatierra, J. Wagner, J.K. Klint, G.F. King, B.M. Olivera, and F. Bosmans. 2015. From foe to friend: using animal toxins to investigate ion channel function. *J. Mol. Biol.* 427:158–175. <https://doi.org/10.1016/j.jmb.2014.07.027>
- Kim, S.E., A. Patapoutian, and J. Grandl. 2013. Single residues in the outer pore of TRPV1 and TRPV3 have temperature-dependent conformations. *PLoS One*. 8:e59593. <https://doi.org/10.1371/journal.pone.0059593>
- Kitaguchi, T., and K.J. Swartz. 2005. An inhibitor of TRPV1 channels isolated from funnel Web spider venom. *Biochemistry*. 44:15544–15549. <https://doi.org/10.1021/bi051494l>
- Kuang, Q., P. Purhonen, and H. Hebert. 2015. Structure of potassium channels. *Cell. Mol. Life Sci.* 72:3677–3693. <https://doi.org/10.1007/s00018-015-1948-5>
- Kühlbrandt, W. 2014. Biochemistry. The resolution revolution. *Science*. 343:1443–1444. <https://doi.org/10.1126/science.1251652>
- Labro, A.J., and D.J. Snyders. 2012. Being flexible: the voltage-controllable activation gate of kv channels. *Front. Pharmacol.* 3:168. <https://doi.org/10.3389/fphar.2012.00168>
- Ladrón-de-Guevara, E., L. Dominguez, G.E. Rangel-Yescas, D.A. Fernández-Velasco, A. Torres-Larios, T. Rosenbaum, and L.D. Islas. 2019. The Contribution of the Ankyrin Repeat Domain of TRPV1 as a Thermal Module. *Biophys. J.* <https://doi.org/10.1016/j.bpj.2019.10.041>
- Lambers, T.T., A.F. Weidema, B. Nilius, J.G. Hoenderop, and R.J. Bindels. 2004. Regulation of the mouse epithelial Ca₂(+) channel TRPV6 by the Ca₂(+)-sensor calmodulin. *J. Biol. Chem.* 279:28855–28861. <https://doi.org/10.1074/jbc.M313637200>
- Launay, P., A. Fleig, A.L. Perraud, A.M. Scharenberg, R. Penner, and J.P. Kinet. 2002. TRPM4 is a Ca₂+-activated nonselective cation channel mediating cell membrane depolarization. *Cell*. 109:397–407. [https://doi.org/10.1016/S0092-8674\(02\)00719-5](https://doi.org/10.1016/S0092-8674(02)00719-5)
- Laursen, W.J., E.R. Schneider, D.K. Merriman, S.N. Bagriantsev, and E.O. Gracheva. 2016. Low-cost functional plasticity of TRPV1 supports heat tolerance in squirrels and camels. *Proc. Natl. Acad. Sci. USA*. 113:11342–11347. <https://doi.org/10.1073/pnas.1604269113>
- Lee, S.Y., and R. MacKinnon. 2004. A membrane-access mechanism of ion channel inhibition by voltage sensor toxins from spider venom. *Nature*. 430:232–235. <https://doi.org/10.1038/nature02632>
- Lepault, J., F.P. Booy, and J. Dubochet. 1983. Electron microscopy of frozen biological suspensions. *J. Microsc.* 129:89–102. <https://doi.org/10.1111/j.1365-2818.1983.tb04163.x>
- Li, X., P. Mooney, S. Zheng, C.R. Booth, M.B. Braunfeld, S. Gubbens, D.A. Agard, and Y. Cheng. 2013. Electron counting and beam-induced motion correction enable near-atomic-resolution single-particle cryo-EM. *Nat. Methods*. 10:584–590. <https://doi.org/10.1038/nmeth.2472>
- Li, Q., S. Wanderling, M. Paduch, D. Medovoy, A. Singharoy, R. McGreevy, C.A. Villalba-Galea, R.E. Hulse, B. Roux, K. Schulten, et al. 2014. Structural mechanism of voltage-dependent gating in an isolated voltage-sensing domain. *Nat. Struct. Mol. Biol.* 21:244–252. <https://doi.org/10.1038/nsmb.2768>
- Li, M., W.K. Zhang, N.M. Benveniste, X. Zhou, D. Su, H. Li, S. Wang, I.E. Michailidis, L. Tong, X. Li, and J. Yang. 2017. Structural basis of dual Ca²⁺/pH regulation of the endolysosomal TRPML1 channel. *Nat. Struct. Mol. Biol.* 24:205–213. <https://doi.org/10.1038/nsmb.3362>
- Liao, M., E. Cao, D. Julius, and Y. Cheng. 2013. Structure of the TRPV1 ion channel determined by electron cryo-microscopy. *Nature*. 504:107–112. <https://doi.org/10.1038/nature12822>
- Liedtke, W., Y. Choe, M.A. Martí-Renom, A.M. Bell, C.S. Denis, A. Sali, A.J. Hudspeth, J.M. Friedman, and S. Heller. 2000. Vanilloid receptor-related osmotically activated channel (VR-OAC), a candidate vertebrate osmoreceptor. *Cell*. 103:525–535. [https://doi.org/10.1016/S0092-8674\(00\)00143-4](https://doi.org/10.1016/S0092-8674(00)00143-4)
- Liu, D., and E.R. Liman. 2003. Intracellular Ca²⁺ and the phospholipid PIP₂ regulate the taste transduction ion channel TRPM5. *Proc. Natl. Acad. Sci. USA*. 100:15160–15165. <https://doi.org/10.1073/pnas.2334159100>
- Liu, B., and F. Qin. 2017. Single-residue molecular switch for high-temperature dependence of vanilloid receptor TRPV3. *Proc. Natl. Acad. Sci. USA*. 114:1589–1594. <https://doi.org/10.1073/pnas.1615304114>
- Liu, C.H., T. Wang, M. Postma, A.G. Obukhov, C. Montell, and R.C. Hardie. 2007. In vivo identification and manipulation of the Ca₂+ selectivity filter in the Drosophila transient receptor potential channel. *J. Neurosci.* 27:604–615. <https://doi.org/10.1523/JNEUROSCI.4099-06.2007>
- Long, S.B., E.B. Campbell, and R. MacKinnon. 2005a. Crystal structure of a mammalian voltage-dependent Shaker family K⁺ channel. *Science*. 309:897–903. <https://doi.org/10.1126/science.1116269>
- Long, S.B., E.B. Campbell, and R. MacKinnon. 2005b. Voltage sensor of Kv1.2: structural basis of electromechanical coupling. *Science*. 309:903–908. <https://doi.org/10.1126/science.1116270>
- Long, S.B., X. Tao, E.B. Campbell, and R. MacKinnon. 2007. Atomic structure of a voltage-dependent K⁺ channel in a lipid membrane-like environment. *Nature*. 450:376–382. <https://doi.org/10.1038/nature06265>
- Matta, J.A., and G.P. Ahern. 2007. Voltage is a partial activator of rat thermosensitive TRP channels. *J. Physiol.* 585:469–482. <https://doi.org/10.1113/jphysiol.2007.144287>
- McGoldrick, L.L., A.K. Singh, K. Saotome, M.V. Yelshanskaya, E.C. Twomey, R.A. Grassucci, and A.I. Sobolevsky. 2018. Opening of the human epithelial calcium channel TRPV6. *Nature*. 553:233–237. <https://doi.org/10.1038/nature25182>
- McKemy, D.D., W.M. Neuhauser, and D. Julius. 2002. Identification of a cold receptor reveals a general role for TRP channels in thermosensation. *Nature*. 416:52–58. <https://doi.org/10.1038/nature719>
- McMullan, G., A.R. Faruqi, D. Clare, and R. Henderson. 2014. Comparison of optimal performance at 300keV of three direct electron detectors for use in low dose electron microscopy. *Ultramicroscopy*. 147:156–163. <https://doi.org/10.1016/j.ultramic.2014.08.002>
- McMullan, G., A.R. Faruqi, and R. Henderson. 2016. Direct Electron Detectors. *Methods Enzymol.* 579:1–17. <https://doi.org/10.1016/bs.mie.2016.05.056>
- Melnick, C., and M. Kaviany. 2018. Thermal actuation in TRPV1: Role of embedded lipids and intracellular domains. *J. Theor. Biol.* 444:38–49. <https://doi.org/10.1016/j.jtbi.2018.02.004>
- Montell, C. 2012. Drosophila visual transduction. *Trends Neurosci.* 35:356–363. <https://doi.org/10.1016/j.tins.2012.03.004>
- Myers, B.R., C.J. Bohlen, and D. Julius. 2008. A yeast genetic screen reveals a critical role for the pore helix domain in TRP channel gating. *Neuron*. 58:362–373. <https://doi.org/10.1016/j.neuron.2008.04.012>

- Nakane, T., D. Kimanius, E. Lindahl, and S.H. Scheres. 2018. Characterisation of molecular motions in cryo-EM single-particle data by multi-body refinement in RELION. *eLife*. 7:e36861. <https://doi.org/10.7554/eLife.36861>
- Neyton, J., and C. Miller. 1988. Discrete Ba²⁺ block as a probe of ion occupancy and pore structure in the high-conductance Ca²⁺-activated K⁺ channel. *J. Gen. Physiol.* 92:569–586. <https://doi.org/10.1085/jgp.92.5.569>
- Ng, L.C.T., T.N. Vien, V. Yarov-Yarovoy, and P.G. DeCaen. 2019. Opening TRPP2 (PKD2L1) requires the transfer of gating charges. *Proc. Natl. Acad. Sci. USA*. 116:15540–15549. <https://doi.org/10.1073/pnas.1902917116>
- Nilius, B., R. Vennekens, J. Prenen, J.G. Hoenderop, G. Droogmans, and R.J. Bindels. 2001. The single pore residue Asp542 determines Ca²⁺ permeation and Mg²⁺ block of the epithelial Ca²⁺ channel. *J. Biol. Chem.* 276:1020–1025. <https://doi.org/10.1074/jbc.M006184200>
- Nilius, B., F. Weidema, J. Prenen, J.G. Hoenderop, R. Vennekens, S. Hoefs, G. Droogmans, and R.J. Bindels. 2003. The carboxyl terminus of the epithelial Ca(2+) channel ECaCl1 is involved in Ca(2+)-dependent inactivation. *Pflugers Arch.* 445:584–588. <https://doi.org/10.1007/s00424-002-0923-9>
- Nilius, B., J. Prenen, A. Janssens, G. Owsianik, C. Wang, M.X. Zhu, and T. Voets. 2005. The selectivity filter of the cation channel TRPM4. *J. Biol. Chem.* 280:22899–22906. <https://doi.org/10.1074/jbc.M501686200>
- Noskov, S.Y., S. Bernèche, and B. Roux. 2004. Control of ion selectivity in potassium channels by electrostatic and dynamic properties of carbonyl ligands. *Nature*. 431:830–834. <https://doi.org/10.1038/nature02943>
- Numazaki, M., T. Tominaga, H. Toyooka, and M. Tominaga. 2002. Direct phosphorylation of capsaicin receptor VR1 by protein kinase Cepsilon and identification of two target serine residues. *J. Biol. Chem.* 277:13375–13378. <https://doi.org/10.1074/jbc.C200104200>
- Oseguera, A.J., L.D. Islas, R. García-Villegas, and T. Rosenbaum. 2007. On the mechanism of TBA block of the TRPV1 channel. *Biophys. J.* 92:3901–3914. <https://doi.org/10.1529/biophysj.106.102400>
- Palovcak, E., L. Delemotte, M.L. Klein, and V. Carnevale. 2015. Comparative sequence analysis suggests a conserved gating mechanism for TRP channels. *J. Gen. Physiol.* 146:37–50. <https://doi.org/10.1085/jgp.201411329>
- Pan, X., Z. Li, Q. Zhou, H. Shen, K. Wu, X. Huang, J. Chen, J. Zhang, X. Zhu, J. Lei, et al. 2018. Structure of the human voltage-gated sodium channel Na_v1.4 in complex with β1. *Science*. 362:eaau2486. <https://doi.org/10.1126/science.aau2486>
- Pan, X., Z. Li, X. Huang, G. Huang, S. Gao, H. Shen, L. Liu, J. Lei, and N. Yan. 2019. Molecular basis for pore blockade of human Na⁺ channel Na_v1.2 by the μ-conotoxin KIIIA. *Science*. 363:1309–1313. <https://doi.org/10.1126/science.aaw2999>
- Paulsen, C.E., J.P. Armache, Y. Gao, Y. Cheng, and D. Julius. 2015. Structure of the TRPA1 ion channel suggests regulatory mechanisms. *Nature*. 525:552. <https://doi.org/10.1038/nature14871>
- Payandeh, J., T. Scheuer, N. Zheng, and W.A. Catterall. 2011. The crystal structure of a voltage-gated sodium channel. *Nature*. 475:353–358. <https://doi.org/10.1038/nature10238>
- Peier, A.M., A. Moqrich, A.C. Hergarden, A.J. Reeve, D.A. Andersson, G.M. Story, T.J. Earley, I. Dragoni, P. McIntyre, S. Bevan, and A. Patapoutian. 2002a. A TRP channel that senses cold stimuli and menthol. *Cell*. 108:705–715. [https://doi.org/10.1016/S0092-8674\(02\)00652-9](https://doi.org/10.1016/S0092-8674(02)00652-9)
- Peier, A.M., A.J. Reeve, D.A. Andersson, A. Moqrich, T.J. Earley, A.C. Hergarden, G.M. Story, S. Colley, J.B. Hogenesch, P. McIntyre, et al. 2002b. A heat-sensitive TRP channel expressed in keratinocytes. *Science*. 296:2046–2049. <https://doi.org/10.1126/science.1073140>
- Phillips, E., A. Reeve, S. Bevan, and P. McIntyre. 2004. Identification of species-specific determinants of the action of the antagonist capsaizine and the agonist PPAHV on TRPV1. *J. Biol. Chem.* 279:17165–17172. <https://doi.org/10.1074/jbc.M313328200>
- Prawitt, D., M.K. Monteilh-Zoller, L. Brixel, C. Spangenberg, B. Zabel, A. Fleig, and R. Penner. 2003. TRPM5 is a transient Ca²⁺-activated cation channel responding to rapid changes in [Ca²⁺]_i. *Proc. Natl. Acad. Sci. USA*. 100:15166–15171. <https://doi.org/10.1073/pnas.2334624100>
- Premkumar, L.S., and G.P. Ahern. 2000. Induction of vanilloid receptor channel activity by protein kinase C. *Nature*. 408:985–990. <https://doi.org/10.1038/35050121>
- Pumroy, R.A., A. Samanta, Y. Liu, T.E. Hughes, S. Zhao, Y. Yudin, T. Rohacs, S. Han, and V.Y. Moiseenkova-Bell. 2019. Molecular mechanism of TRPV2 channel modulation by cannabidiol. *eLife*. 8:e48792. <https://doi.org/10.7554/eLife.48792>
- Punjani, A., J.L. Rubinstein, D.J. Fleet, and M.A. Brubaker. 2017. cryoSPARC: algorithms for rapid unsupervised cryo-EM structure determination. *Nat. Methods*. 14:290–296. <https://doi.org/10.1038/nmeth.4169>
- Ramsey, I.S., M. Delling, and D.E. Clapham. 2006. An introduction to TRP channels. *Annu. Rev. Physiol.* 68:619–647. <https://doi.org/10.1146/annurev.physiol.68.040204.100431>
- Ren, D., B. Navarro, H. Xu, L. Yue, Q. Shi, and D.E. Clapham. 2001. A prokaryotic voltage-gated sodium channel. *Science*. 294:2372–2375. <https://doi.org/10.1126/science.1065635>
- Rettig, J., S.H. Heinemann, F. Wunder, C. Lorra, D.N. Parcej, J.O. Dolly, and O. Pongs. 1994. Inactivation properties of voltage-gated K⁺ channels altered by presence of beta-subunit. *Nature*. 369:289–294. <https://doi.org/10.1038/369289a0>
- Ryu, S., B. Liu, J. Yao, Q. Fu, and F. Qin. 2007. Uncoupling proton activation of vanilloid receptor TRPV1. *J. Neurosci.* 27:12797–12807. <https://doi.org/10.1523/JNEUROSCI.2324-07.2007>
- Sakipov, S., A.I. Sobolevsky, and M.G. Kurnikova. 2018. Ion Permeation Mechanism in Epithelial Calcium Channel TRPV6. *Sci. Rep.* 8:5715. <https://doi.org/10.1038/s41598-018-23972-5>
- Salazar, H., A. Jara-Oseguera, E. Hernández-García, I. Llorente, I.I. Arias-Olguín, M. Soriano-García, L.D. Islas, and T. Rosenbaum. 2009. Structural determinants of gating in the TRPV1 channel. *Nat. Struct. Mol. Biol.* 16:704–710. <https://doi.org/10.1038/nsmb.1633>
- Sánchez-Moreno, A., E. Guevara-Hernández, R. Contreras-Cervera, G. Rangel-Yescas, E. Ladrón-de-Guevara, T. Rosenbaum, and L.D. Islas. 2018. Irreversible temperature gating in trpv1 sheds light on channel activation. *eLife*. 7:e36372. <https://doi.org/10.7554/eLife.36372>
- Saotome, K., A.K. Singh, M.V. Yelshanskaya, and A.I. Sobolevsky. 2016. Crystal structure of the epithelial calcium channel TRPV6. *Nature*. 534:506–511. <https://doi.org/10.1038/nature17975>
- Saxton, W.O., and J. Frank. 1977. Motif detection in quantum noise-limited electron micrographs by cross-correlation. *Ultramicroscopy*. 2:219–227. [https://doi.org/10.1016/S0304-3991\(76\)91385-1](https://doi.org/10.1016/S0304-3991(76)91385-1)
- Scheres, S.H. 2012. RELION: implementation of a Bayesian approach to cryo-EM structure determination. *J. Struct. Biol.* 180:519–530. <https://doi.org/10.1016/j.jsb.2012.09.006>
- Schmiege, P., M. Fine, G. Blobel, and X. Li. 2017. Human TRPML1 channel structures in open and closed conformations. *Nature*. 550:366–370. <https://doi.org/10.1038/nature24036>
- Schoppa, N.E., K. McCormack, M.A. Tanouye, and F.J. Sigworth. 1992. The size of gating charge in wild-type and mutant Shaker potassium channels. *Science*. 255:1712–1715. <https://doi.org/10.1126/science.1553560>
- Shen, P.S., X. Yang, P.G. DeCaen, X. Liu, D. Bulkeley, D.E. Clapham, and E. Cao. 2016. The Structure of the Polycystic Kidney Disease Channel PKD2 in Lipid Nanodiscs. *Cell*. 167:763–773.e11.
- Shen, H., Q. Zhou, X. Pan, Z. Li, J. Wu, and N. Yan. 2017. Structure of a eukaryotic voltage-gated sodium channel at near-atomic resolution. *Science*. 355:eaal4326. <https://doi.org/10.1126/science.aal4326>
- Shen, H., Z. Li, Y. Jiang, X. Pan, J. Wu, B. Cristofori-Armstrong, J.J. Smith, Y.K.Y. Chin, J. Lei, Q. Zhou, et al. 2018. Structural basis for the modulation of voltage-gated sodium channels by animal toxins. *Science*. 362:eaau2596. <https://doi.org/10.1126/science.aau2596>
- Shen, H., D. Liu, K. Wu, J. Lei, and N. Yan. 2019. Structures of human Na_v1.7 channel in complex with auxiliary subunits and animal toxins. *Science*. 363:1303–1308. <https://doi.org/10.1126/science.aaw2493>
- Siemens, J., S. Zhou, R. Piskorowski, T. Nikai, E.A. Lumpkin, A.I. Basbaum, D. King, and D. Julius. 2006. Spider toxins activate the capsaicin receptor to produce inflammatory pain. *Nature*. 444:208–212. <https://doi.org/10.1038/nature05285>
- Sierra-Valdez, F., C.M. Azumaya, L.O. Romero, T. Nakagawa, and J.F. Cordeiro-Morales. 2018. Structure-function analyses of the ion channel TRPC3 reveal that its cytoplasmic domain allosterically modulates channel gating. *J. Biol. Chem.* 293:16102–16114. <https://doi.org/10.1074/jbc.RA118.005066>
- Singh, A.K., K. Saotome, and A.I. Sobolevsky. 2017. Swapping of transmembrane domains in the epithelial calcium channel TRPV6. *Sci. Rep.* 7:10669. <https://doi.org/10.1038/s41598-017-10993-9>
- Singh, A.K., L.L. McGoldrick, and A.I. Sobolevsky. 2018a. Structure and gating mechanism of the transient receptor potential channel TRPV3. *Nat. Struct. Mol. Biol.* 25:805–813. <https://doi.org/10.1038/s41594-018-0108-7>
- Singh, A.K., L.L. McGoldrick, E.C. Twomey, and A.I. Sobolevsky. 2018b. Mechanism of calmodulin inactivation of the calcium-selective TRP channel TRPV6. *Sci Adv.* 4:eaau6088.

- Singh, A.K., K. Saotome, L.L. McGoldrick, and A.I. Sobolevsky. 2018c. Structural bases of TRP channel TRPV6 allosteric modulation by 2-APB. *Nat. Commun.* 9:2465. <https://doi.org/10.1038/s41467-018-04828-y>
- Singh, A.K., L.L. McGoldrick, L. Demirkhanyan, M. Leslie, E. Zakharian, and A.I. Sobolevsky. 2019. Structural basis of temperature sensation by the TRP channel TRPV3. *Nat. Struct. Mol. Biol.* 26:994–998. <https://doi.org/10.1038/s41594-019-0318-7>
- Smith, G.D., M.J. Gunthorpe, R.E. Kelsell, P.D. Hayes, P. Reilly, P. Facer, J.E. Wright, J.C. Jerman, J.P. Walhin, L. Ooi, et al. 2002. TRPV3 is a temperature-sensitive vanilloid receptor-like protein. *Nature*. 418: 186–190. <https://doi.org/10.1038/nature00894>
- Soler-Llavina, G.J., T.H. Chang, and K.J. Swartz. 2006. Functional interactions at the interface between voltage-sensing and pore domains in the Shaker K(v) channel. *Neuron*. 52:623–634. <https://doi.org/10.1016/j.neuron.2006.10.005>
- Song, K., H. Wang, G.B. Kamm, J. Pohle, F.C. Reis, P. Heppenstall, H. Wende, and J. Siemens. 2016. The TRPM2 channel is a hypothalamic heat sensor that limits fever and can drive hypothermia. *Science*. 353:1393–1398. <https://doi.org/10.1126/science.aaf7537>
- Sosa-Pagán, J.O., E.S. Iversen, and J. Grandl. 2017. TRPV1 temperature activation is specifically sensitive to strong decreases in amino acid hydrophobicity. *Sci. Rep.* 7:549. <https://doi.org/10.1038/s41598-017-00636-4>
- Stephens, R.F., W. Guan, B.S. Zhorov, and J.D. Spafford. 2015. Selectivity filters and cysteine-rich extracellular loops in voltage-gated sodium, calcium, and NALCN channels. *Front. Physiol.* 6:153. <https://doi.org/10.3389/fphys.2015.00153>
- Story, G.M., A.M. Peier, A.J. Reeve, S.R. Eid, J. Mosbacher, T.R. Hricik, T.J. Earley, A.C. Hergarden, D.A. Andersson, S.W. Hwang, et al. 2003. ANKTM1, a TRP-like channel expressed in nociceptive neurons, is activated by cold temperatures. *Cell*. 112:819–829. [https://doi.org/10.1016/S0092-8674\(03\)00158-2](https://doi.org/10.1016/S0092-8674(03)00158-2)
- Stuart, D.I., S. Subramaniam, and N.G. Abrescia. 2016. The democratization of cryo-EM. *Nat. Methods*. 13:607–608. <https://doi.org/10.1038/nmeth.3946>
- Su, Q., F. Hu, X. Ge, J. Lei, S. Yu, T. Wang, Q. Zhou, C. Mei, and Y. Shi. 2018a. Structure of the human PKD1-PKD2 complex. *Science*. 361:eaat9819. <https://doi.org/10.1126/science.aat9819>
- Su, Q., F. Hu, Y. Liu, X. Ge, C. Mei, S. Yu, A. Shen, Q. Zhou, C. Yan, J. Lei, et al. 2018b. Cryo-EM structure of the polycystic kidney disease-like channel PKD2L1. *Nat. Commun.* 9:1192. <https://doi.org/10.1038/s41467-018-03606-0>
- Suo, Y., Z. Wang, L. Zubcevic, A.L. Hsu, Q. He, M.J. Borgnia, R.-R. Ji, and S.-Y. Lee. 2019. Structural Insights into Electrophile Irritant Sensing by the Human TRPA1 Channel. *Neuron*. <https://doi.org/10.1016/j.neuron.2019.11.023>
- Talavera, K., K. Yasumatsu, T. Voets, G. Droogmans, N. Shigemura, Y. Ni-nomiya, R.F. Margolske, and B. Nilius. 2005. Heat activation of TRPM5 underlies thermal sensitivity of sweet taste. *Nature*. 438:1022–1025. <https://doi.org/10.1038/nature04248>
- Tan, C.H., and P.A. McNaughton. 2016. The TRPM2 ion channel is required for sensitivity to warmth. *Nature*. 536:460–463. <https://doi.org/10.1038/nature19074>
- Tang, G., L. Peng, P.R. Baldwin, D.S. Mann, W. Jiang, I. Rees, and S.J. Ludtke. 2007. EMAN2: an extensible image processing suite for electron microscopy. *J. Struct. Biol.* 157:38–46. <https://doi.org/10.1016/j.jsb.2006.05.009>
- Tang, L., T.M. Gamal El-Din, J. Payandeh, G.Q. Martinez, T.M. Heard, T. Scheuer, N. Zheng, and W.A. Catterall. 2014. Structural basis for Ca²⁺ selectivity of a voltage-gated calcium channel. *Nature*. 505:56–61. <https://doi.org/10.1038/nature12775>
- Tang, L., T.M. Gamal El-Din, T.M. Swanson, D.C. Pryde, T. Scheuer, N. Zheng, and W.A. Catterall. 2016. Structural basis for inhibition of a voltage-gated Ca²⁺ channel by Ca²⁺ antagonist drugs. *Nature*. 537:117–121. <https://doi.org/10.1038/nature19102>
- Tang, Q., W. Guo, L. Zheng, J.X. Wu, M. Liu, X. Zhou, X. Zhang, and L. Chen. 2018. Structure of the receptor-activated human TRPC6 and TRPC3 ion channels. *Cell Res.* 28:746–755. <https://doi.org/10.1038/s41422-018-0038-2>
- Tao, X., A. Lee, W. Limapichat, D.A. Dougherty, and R. MacKinnon. 2010. A gating charge transfer center in voltage sensors. *Science*. 328:67–73. <https://doi.org/10.1126/science.1185954>
- Ufret-Vincenty, C.A., R.M. Klein, M.D. Collins, M.G. Rosasco, G.Q. Martinez, and S.E. Gordon. 2015. Mechanism for phosphoinositide selectivity and activation of TRPV1 ion channels. *J. Gen. Physiol.* 145:431–442. <https://doi.org/10.1085/jgp.201511354>
- Vandewauw, I., K. De Clercq, M. Mulier, K. Held, S. Pinto, N. Van Ranst, A. Segal, T. Voet, R. Vennekens, K. Zimmermann, et al. 2018. A TRP channel trio mediates acute noxious heat sensing. *Nature*. 555:662–666. <https://doi.org/10.1038/nature26137>
- Vargas, E., V. Yarov-Yarovoy, F. Khalili-Araghi, W.A. Catterall, M.L. Klein, M. Tarek, E. Lindahl, K. Schulten, E. Perozo, F. Bezanilla, and B. Roux. 2012. An emerging consensus on voltage-dependent gating from computational modeling and molecular dynamics simulations. *J. Gen. Physiol.* 140:587–594. <https://doi.org/10.1085/jgp.201210873>
- Venkatachalam, K., and C. Montell. 2007. TRP channels. *Annu. Rev. Biochem.* 76: 387–417. <https://doi.org/10.1146/annurev.biochem.75.103004.142819>
- Vennekens, R., J.G. Hoenderop, J. Prenen, M. Stuijver, P.H. Willems, G. Droogmans, B. Nilius, and R.J. Bindels. 2000. Permeation and gating properties of the novel epithelial Ca(2+) channel. *J. Biol. Chem.* 275: 3963–3969. <https://doi.org/10.1074/jbc.275.6.3963>
- Vieira-Pires, R.S., and J.H. Morais-Cabral. 2010. 3(10) helices in channels and other membrane proteins. *J. Gen. Physiol.* 136:585–592. <https://doi.org/10.1085/jgp.201010508>
- Vinayagam, D., T. Mager, A. Apelbaum, A. Bothe, F. Merino, O. Hofnagel, C. Gatsogiannis, and S. Raunser. 2018. Electron cryo-microscopy structure of the canonical TRPC4 ion channel. *eLife*. 7:e36615. <https://doi.org/10.7554/eLife.36615>
- Viswanath, V., G.M. Story, A.M. Peier, M.J. Petrus, V.M. Lee, S.W. Hwang, A. Patapoutian, and T. Jegla. 2003. Opposite thermosensor in fruitfly and mouse. *Nature*. 423:822–823. <https://doi.org/10.1038/423822a>
- Voets, T., J. Prenen, J. Vriens, H. Watanabe, A. Janssens, U. Wissenbach, M. Bödding, G. Droogmans, and B. Nilius. 2002. Molecular determinants of permeation through the cation channel TRPV4. *J. Biol. Chem.* 277: 33704–33710. <https://doi.org/10.1074/jbc.M204828200>
- Voets, T., G. Droogmans, U. Wissenbach, A. Janssens, V. Flockerzi, and B. Nilius. 2004a. The principle of temperature-dependent gating in cold- and heat-sensitive TRP channels. *Nature*. 430:748–754. <https://doi.org/10.1038/nature02732>
- Voets, T., A. Janssens, G. Droogmans, and B. Nilius. 2004b. Outer pore architecture of a Ca²⁺-selective TRP channel. *J. Biol. Chem.* 279: 15223–15230. <https://doi.org/10.1074/jbc.M312076200>
- Vriens, J., G. Owsianik, T. Hofmann, S.E. Philipp, J. Stab, X. Chen, M. Benoit, F. Xue, A. Janssens, S. Kerselaers, et al. 2011. TRPM3 is a nociceptor channel involved in the detection of noxious heat. *Neuron*. 70:482–494. <https://doi.org/10.1016/j.neuron.2011.02.051>
- Wang, G., Y.T. Qiu, T. Lu, H.W. Kwon, R.J. Pitts, J.J. Van Loon, W. Takken, and L.J. Zwiebel. 2009. Anopheles gambiae TRPA1 is a heat-activated channel expressed in thermosensitive sensilla of female antennae. *Eur. J. Neurosci.* 30:967–974. <https://doi.org/10.1111/j.1460-9568.2009.06901.x>
- Wang, L., T.M. Fu, Y. Zhou, S. Xia, A. Greka, and H. Wu. 2018. Structures and gating mechanism of human TRPM2. *Science*. 362:eaav4809. <https://doi.org/10.1126/science.aav4809>
- Wen, H., and W. Zheng. 2018. Decrypting the Heat Activation Mechanism of TRPV1 Channel by Molecular Dynamics Simulation. *Biophys. J.* 114: 40–52. <https://doi.org/10.1016/j.bpj.2017.10.034>
- Wen, H., F. Qin, and W. Zheng. 2016. Toward elucidating the heat activation mechanism of the TRPV1 channel gating by molecular dynamics simulation. *Proteins*. 84:1938–1949. <https://doi.org/10.1002/prot.25177>
- Wilkes, M., M.G. Madej, L. Kreuter, D. Rhinow, V. Heinz, S. De Sanctis, S. Ruppel, R.M. Richter, F. Joos, M. Grieben, et al. 2017. Molecular insights into lipid-assisted Ca²⁺ regulation of the TRP channel Polycystin-2. *Nat. Struct. Mol. Biol.* 24:123–130. <https://doi.org/10.1038/nsmb.3357>
- Winkler, P.A., Y. Huang, W. Sun, J. Du, and W. Lü. 2017. Electron cryo-microscopy structure of a human TRPM4 channel. *Nature*. 552: 200–204. <https://doi.org/10.1038/nature24674>
- Wu, L.J., T.B. Sweet, and D.E. Clapham. 2010. International Union of Basic and Clinical Pharmacology. LXXVI. Current progress in the mammalian TRP ion channel family. *Pharmacol. Rev.* 62:381–404. <https://doi.org/10.1124/pr.110.002725>
- Wu, J., Z. Yan, Z. Li, X. Qian, S. Lu, M. Dong, Q. Zhou, and N. Yan. 2016. Structure of the voltage-gated calcium channel Ca(v)1.1 at 3.6 Å resolution. *Nature*. 537:191–196. <https://doi.org/10.1038/nature19321>
- Xu, H., I.S. Ramsey, S.A. Kotecha, M.M. Moran, J.A. Chong, D. Lawson, P. Ge, J. Lilly, I. Silos-Santiago, Y. Xie, et al. 2002. TRPV3 is a calcium-permeable temperature-sensitive cation channel. *Nature*. 418:181–186. <https://doi.org/10.1038/nature00882>

- Xu, S.Z., P. Sukumar, F. Zeng, J. Li, A. Jairaman, A. English, J. Naylor, C. Ciurtin, Y. Majeed, C.J. Milligan, et al. 2008. TRPC channel activation by extracellular thioredoxin. *Nature*. 451:69–72. <https://doi.org/10.1038/nature06414>
- Xu, H., T. Li, A. Rohou, C.P. Arthur, F. Tzakoniati, E. Wong, A. Estevez, C. Kugel, Y. Franke, J. Chen, et al. 2019. Structural Basis of Nav1.7 Inhibition by a Gating-Modifier Spider Toxin. *Cell*. 176:702–715.
- Yan, Z., Q. Zhou, L. Wang, J. Wu, Y. Zhao, G. Huang, W. Peng, H. Shen, J. Lei, and N. Yan. 2017. Structure of the Nav1.4-beta1 Complex from Electric Eel. *Cell*. 170:470–482.
- Yang, F., Y. Cui, K. Wang, and J. Zheng. 2010. Thermosensitive TRP channel pore turret is part of the temperature activation pathway. *Proc. Natl. Acad. Sci. USA*. 107:7083–7088. <https://doi.org/10.1073/pnas.1000357107>
- Yang, F., X. Xiao, W. Cheng, W. Yang, P. Yu, Z. Song, V. Yarov-Yarovoy, and J. Zheng. 2015a. Structural mechanism underlying capsaicin binding and activation of the TRPV1 ion channel. *Nat. Chem. Biol.* 11:518–524. <https://doi.org/10.1038/nchembio.1835>
- Yang, S., F. Yang, N. Wei, J. Hong, B. Li, L. Luo, M. Rong, V. Yarov-Yarovoy, J. Zheng, K. Wang, and R. Lai. 2015b. A pain-inducing centipede toxin targets the heat activation machinery of nociceptor TRPV1. *Nat. Commun.* 6:8297. <https://doi.org/10.1038/ncomms9297>
- Yang, F., S. Vu, V. Yarov-Yarovoy, and J. Zheng. 2016. Rational design and validation of a vanilloid-sensitive TRPV2 ion channel. *Proc. Natl. Acad. Sci. USA*. 113:E3657–E3666. <https://doi.org/10.1073/pnas.1604180113>
- Yang, F., X. Xiao, B.H. Lee, S. Vu, W. Yang, V. Yarov-Yarovoy, and J. Zheng. 2018. The conformational wave in capsaicin activation of transient receptor potential vanilloid 1 ion channel. *Nat. Commun.* 9:2879. <https://doi.org/10.1038/s41467-018-05339-6>
- Yao, J., B. Liu, and F. Qin. 2010. Pore turret of thermal TRP channels is not essential for temperature sensing. *Proc. Natl. Acad. Sci. USA*. 107:E125, author reply E126–E127. <https://doi.org/10.1073/pnas.1008272107>
- Yao, J., B. Liu, and F. Qin. 2011. Modular thermal sensors in temperature-gated transient receptor potential (TRP) channels. *Proc. Natl. Acad. Sci. USA*. 108:11109–11114. <https://doi.org/10.1073/pnas.1105196108>
- Yeh, B.I., Y.K. Kim, W. Jabbar, and C.L. Huang. 2005. Conformational changes of pore helix coupled to gating of TRPV5 by protons. *EMBO J.* 24:3224–3234. <https://doi.org/10.1038/sj.emboj.7600795>
- Yin, Y., M. Wu, L. Zubcevic, W.F. Borschel, G.C. Lander, and S.Y. Lee. 2018. Structure of the cold- and menthol-sensing ion channel TRPM8. *Science*. 359:237–241. <https://doi.org/10.1126/science.aan4325>
- Yin, Y., S.C. Le, A.L. Hsu, M.J. Borgnia, H. Yang, and S.Y. Lee. 2019a. Structural basis of cooling agent and lipid sensing by the cold-activated TRPM8 channel. *Science*. 363:eaav9334. <https://doi.org/10.1126/science.aav9334>
- Yin, Y., M. Wu, A.L. Hsu, W.F. Borschel, M.J. Borgnia, G.C. Lander, and S.Y. Lee. 2019b. Visualizing structural transitions of ligand-dependent gating of the TRPM2 channel. *Nat. Commun.* 10:3740. <https://doi.org/10.1038/s41467-019-11733-5>
- Yue, L., J.B. Peng, M.A. Hediger, and D.E. Clapham. 2001. CaT1 manifests the pore properties of the calcium-release-activated calcium channel. *Nature*. 410:705–709. <https://doi.org/10.1038/35070596>
- Zagotta, W.N., T. Hoshi, and R.W. Aldrich. 1990. Restoration of inactivation in mutants of Shaker potassium channels by a peptide derived from ShB. *Science*. 250:568–571. <https://doi.org/10.1126/science.2122520>
- Zagotta, W.N., M.T. Gordon, E.N. Senning, M.A. Munari, and S.E. Gordon. 2016. Measuring distances between TRPV1 and the plasma membrane using a noncanonical amino acid and transition metal ion FRET. *J. Gen. Physiol.* 147:201–216. <https://doi.org/10.1085/jgp.201511531>
- Zhang, X., L. Jin, Q. Fang, W.H. Hui, and Z.H. Zhou. 2010. 3.3 Å cryo-EM structure of a nonenveloped virus reveals a priming mechanism for cell entry. *Cell*. 141:472–482. <https://doi.org/10.1016/j.cell.2010.03.041>
- Zhang, X., W. Ren, P. DeCaen, C. Yan, X. Tao, L. Tang, J. Wang, K. Hasegawa, T. Kumasaka, J. He, et al. 2012. Crystal structure of an orthologue of the NaChBac voltage-gated sodium channel. *Nature*. 486:130–134. <https://doi.org/10.1038/nature11054>
- Zhang, F., S.M. Hanson, A. Jara-Oseguera, D. Krepley, C. Bae, L.V. Pearce, P.M. Blumberg, S. Newstead, and K.J. Swartz. 2016. Engineering vanilloid-sensitivity into the rat TRPV2 channel. *eLife*. 5:e16409. <https://doi.org/10.7554/eLife.16409>
- Zhang, F., A. Jara-Oseguera, T.H. Chang, C. Bae, S.M. Hanson, and K.J. Swartz. 2018a. Heat activation is intrinsic to the pore domain of TRPV1. *Proc. Natl. Acad. Sci. USA*. 115:E317–E324. <https://doi.org/10.1073/pnas.1717192115>
- Zhang, Z., B. Toth, A. Szollosi, J. Chen, and L. Csanady. 2018b. Structure of a TRPM2 channel in complex with Ca²⁺ explains unique gating regulation. *eLife*. 7:e36409.
- Zhang, F., K.J. Swartz, and A. Jara-Oseguera. 2019. Conserved allosteric pathways for activation of TRPV3 revealed through engineering vanilloid-sensitivity. *eLife*. 8:e42756.
- Zhao, J., J.V. Lin King, Y. Cheng, and D. Julius. 2019. Mechanisms governing irritant-evoked activation and calcium modulation of TRPA1. *bioRxiv*. doi:<https://doi.org/10.1101/2019.12.26.888982> (Preprint posted December 27, 2019).
- Zheng, W., and F. Qin. 2015. A combined coarse-grained and all-atom simulation of TRPV1 channel gating and heat activation. *J. Gen. Physiol.* 145:443–456. <https://doi.org/10.1085/jgp.201411335>
- Zheng, W., X. Yang, R. Hu, R. Cai, L. Hofmann, Z. Wang, Q. Hu, X. Liu, D. Bulkeley, Y. Yu, et al. 2018. Hydrophobic pore gates regulate ion permeation in polycystic kidney disease 2 and 2L1 channels. *Nat. Commun.* 9:2302. <https://doi.org/10.1038/s41467-018-04586-x>
- Zhou, M., J.H. Morais-Cabral, S. Mann, and R. MacKinnon. 2001a. Potassium channel receptor site for the inactivation gate and quaternary amine inhibitors. *Nature*. 411:657–661. <https://doi.org/10.1038/35079500>
- Zhou, Y., J.H. Morais-Cabral, A. Kaufman, and R. MacKinnon. 2001b. Chemistry of ion coordination and hydration revealed by a K⁺ channel-Fab complex at 2.0 Å resolution. *Nature*. 414:43–48. <https://doi.org/10.1038/35102009>
- Zhou, X., M. Li, D. Su, Q. Jia, H. Li, X. Li, and J. Yang. 2017. Cryo-EM structures of the human endolysosomal TRPML3 channel in three distinct states. *Nat. Struct. Mol. Biol.* 24:1146–1154. <https://doi.org/10.1038/nsmb.3502>
- Zimmermann, K., J.K. Lennerz, A. Hein, A.S. Link, J.S. Kaczmarek, M. Delling, S. Uysal, J.D. Pfeifer, A. Riccio, and D.E. Clapham. 2011. Transient receptor potential cation channel, subfamily C, member 5 (TRPC5) is a cold-transducer in the peripheral nervous system. *Proc. Natl. Acad. Sci. USA*. 108:18114–18119. <https://doi.org/10.1073/pnas.1115387108>
- Zubcevic, L., and S.Y. Lee. 2019. The role of π -helices in TRP channel gating. *Curr. Opin. Struct. Biol.* 58:314–323. <https://doi.org/10.1016/j.sbi.2019.06.011>
- Zubcevic, L., M.A. Herzik Jr., B.C. Chung, Z. Liu, G.C. Lander, and S.Y. Lee. 2016. Cryo-electron microscopy structure of the TRPV2 ion channel. *Nat. Struct. Mol. Biol.* 23:180–186. <https://doi.org/10.1038/nsmb.3159>
- Zubcevic, L., M.A. Herzik Jr., M. Wu, W.F. Borschel, M. Hirschi, A.S. Song, G.C. Lander, and S.Y. Lee. 2018a. Conformational ensemble of the human TRPV3 ion channel. *Nat. Commun.* 9:4773. <https://doi.org/10.1038/s41467-018-07117-w>
- Zubcevic, L., S. Le, H. Yang, and S.Y. Lee. 2018b. Conformational plasticity in the selectivity filter of the TRPV2 ion channel. *Nat. Struct. Mol. Biol.* 25:405–415. <https://doi.org/10.1038/s41594-018-0059-z>
- Zubcevic, L., W.F. Borschel, A.L. Hsu, M.J. Borgnia, and S.Y. Lee. 2019. Regulatory switch at the cytoplasmic interface controls TRPV channel gating. *eLife*. 8:e47746. <https://doi.org/10.7554/eLife.47746>